Determining the origin and changing shape of landscape-scale rock formations with three-dimensional modelling: The Borologa rock shelters, Kimberley region, Australia

Jean-Jacques Delannoy, Kim Genuite, Jean-jacques Delannoy, Bruno David, Augustine Unghango, Balanggarra Aboriginal Corporation, Gaël Cazes, Reka Fulop, David Fink, Alexandru Codilean, et al.

Author's Accepted manuscript

Geoarchaeology 36(3):1-9. DOI: https://doi.org/10.1002/gea.218632021.

Public, shareable link -

https://onlinelibrary.wiley.com/share/author/3FA9TYF4NZNCQVNQVQV2?target=10.1002/gea.21863

Determining the origin and changing shape of landscape-scale rock formations with three-dimensional modelling: The Borologa rock shelters, Kimberley region, Australia

Kim Genuite[1], Jean-Jacques Delannoy[1,2], Bruno David[2,3], Augustine Unghango[4], Balanggarra Aboriginal Corporation[4], Gaël Cazes[5,6], Reka Fulop[5], David Fink[6], Alexandru Codilean[2,5], Sven Ouzman[7], Peter Veth[7], Sam Harper[7], Helen Green[2,8], Damien Finch[8], Chris Urwin[2,3]

[1] Laboratoire EDYTEM, Université Savoie Mont Blanc, F-73376 Le Bourget du Lac Cedex, France

[2] ARC Centre of Excellence for Australian Biodiversity and Heritage, Canberra, ACT 2601, Australia

[3] Monash Indigenous Studies Centre, 20 Chancellors Walk, Monash University, Clayton campus, VIC 3800, Australia

[4] P.O. Box 372, Wyndham, WA 6740, Australia

[5] Faculty of Science, Medicine and Health, University of Wollongong, Wollongong, NSW 2522, Australia

[6] Australian Nuclear Science and Technology Organisation (ANSTO), Lucas Heights, NSW 2234, Australia

[7] Centre for Rock Art Research + Management, M257, School of Social Sciences, Faculty of Arts, Business, Law and Education, The University of Western Australia, 35 Stirling Highway, Crawley, WA 6009, Australia

[8] School of Earth Sciences, University of Melbourne, Parkville, VIC 3010, Australia

ORCIDs:

Kim Genuite: https://orcid.org/0000-0002-5391-5461

Jean-Jacques Delannoy: ORCID: https://orcid.org/0000-0002-2815-4920

Bruno David: ORCID: https://orcid.org/0000-0002-8567-6135

Gaël Cazes: ORCID: https://orcid.org/0000-0001-7631-1057

Reka Fulop: https://orcid.org/0000-0002-3237-0319

Alexandru Codilean: https://orcid.org/0000-0003-1895-5633

Sven Ouzman: ORCID: https://orcid.org/0000-0002-9379-2996

Peter Veth: ORCID: https://orcid.org/0000-0002-1717-6390

Sam Harper: ORCID: https://orcid.org/0000-0002-1590-2387

Helen Green: ORCID: https://orcid.org/0000-0002-7842-6007

Damien Finch: ORCID: https://orcid.org/0000-0002-9447-5685

Chris Urwin: ORCID: https://orcid.org/0000-0002-3868-9574

Corresponding author: Bruno David, bruno.david@monash.edu

Abstract

Archaeologists often wonder how and when rock shelters formed, yet their origins and antiquity are almost never systematically investigated. Here we present a new method by which to determine how and when individual boulders and rock shelters came to lie in their present landscape settings. We do so through 3D laser (LiDAR) mapping, illustrating the method by example of the Borologa Aboriginal site complex in the Kimberley region of northwestern Australia. Through a combination of geomorphological study and high-resolution 3D modelling, individual blocks of rock are re-fitted and re-positioned onto their originating cliff-line. Preliminary cosmogenic nuclide ages on exposed vertical cliff faces and

associated detached boulders above the Borologa archaeological sites signal very slow detachment rates for the mass movements of large blocks down the Drysdale Valley slopes, suggesting relative landscape stability over hundreds of thousands of years (predating the arrival of people). These findings offer hitherto unknown details of the pace of regional landscape evolution, and move us towards a better understanding of patterns of human occupation in a context of relatively stable rock outcrops both within the sites and across the region.

Keywords: 3D modelling; Aboriginal landscapes; landscape archaeology; LiDAR; Kimberley region; rock shelter formation

1 Introduction

Archaeologists often seek to determine the beginnings of things: when did people first colonise a region? When was a stone artefact type first made? When was a site first used? Those beginnings are then positioned in broader socio-geographical settings, such as to investigate the spread of people across land and seascapes (e.g., for a story of global colonization, see Gamble, 1994); the introduction of artefact types and technologies from one area to another (e.g., for the spread of Sudden and San Rafael Side-notched points along the southern Rocky Mountains, U.S.A., see David et al., 2005); when people started to modify the physical matrix of rock shelters (e.g., in Arnhem Land, Delannoy et al., 2017; in the Kimberley, Delannoy et al., 2020a); or temporal trends in site and regional occupation (e.g., for increased intensities of site use in Late Holocene temperate Australia, see Lourandos, 1983). Rock shelters feature prominently in many such investigations, because their prominent physical demarcation and visibility in the landscape often signal enduring locales of human activity that span thousands of years. However, understanding the first human use

of rock shelters can be compromised by the antiquity of the rock shelters themselves, because their origins as features in the landscape are almost never investigated. Rarely is it known if the start of occupation coincides with a site's formation, or whether a temporal lag existed between a site's formation and its first human occupation. Yet the coincidence, or separation, of the two has significant implications for our ability to understand regional occupation patterns, the scheduling of habitation and resource exploitation, population densities and many other aspects of the human past (e.g., David & Lourandos, 1997). Here we present a method by which to study whether quartzite boulders ("blocks" or "stacks") have been geomorphologically re-located from elsewhere (i.e. as "floats"), and, if so, how and when they attained their present configurations. We illustrate the method through the example of the Borologa rock shelter complex in the Kimberley region of northwestern Australia (Fig. 1).

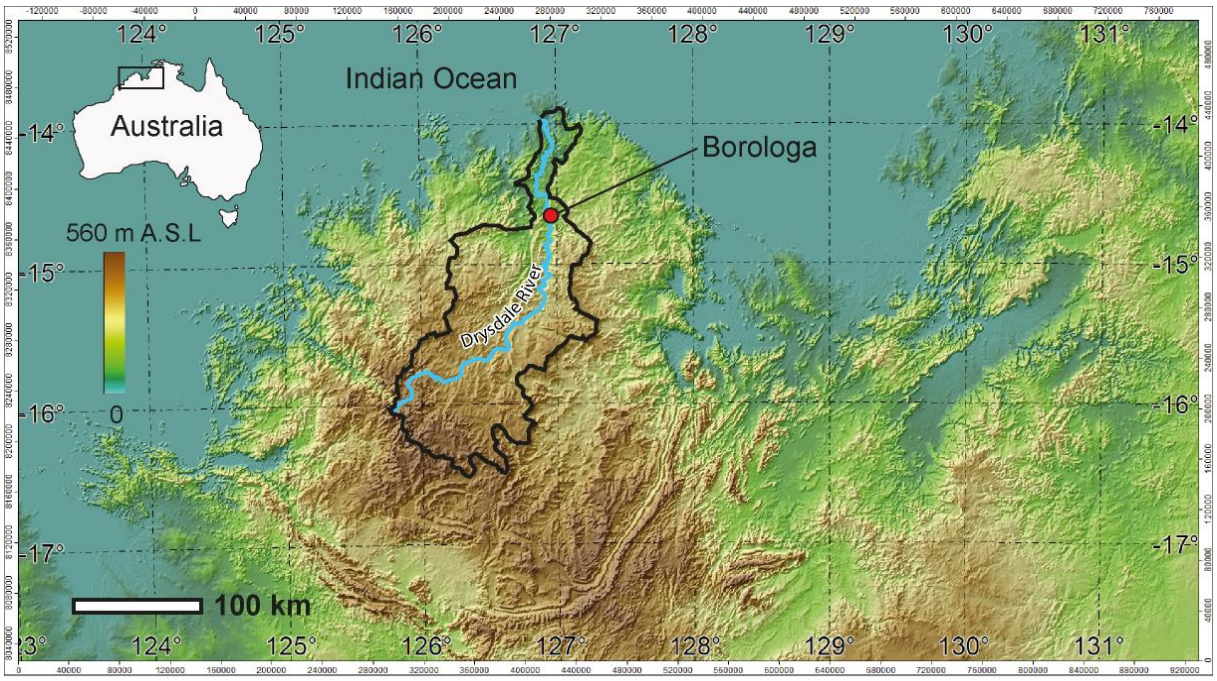

Figure 1. Location of the Borologa site complex and Drysdale River watershed, Kimberley region, northwestern Australia (after Global Multi-resolution Terrain Elevation Data (GMTED) 2010; Danielson & Gesch, 2011).

2 Site setting

Australia's Kimberley region is renowned for its rich Aboriginal heritage, including tens of thousands of rock art sites in quartzite rock shelters and limestone caves. The quartzite shelters are particularly abundant, and come from a variety of geological formations. For example, in the eastern Kimberley, where this research was conducted, 1315 archaeological sites have been located and recorded since 2013 in partnership with the Balanggarra Aboriginal Corporation as part of the *Kimberley Visions: rock art style provinces of northern Australia* Australian Research Council Linkage Project. These sites include open-air quarries; grinding locales; burials; stone arrangements; engraved, painted and marked rock shelters (some with buried archaeological deposits); historic camp sites; ochre sources; and ethnographic sites (Harper et al., 2020). Of these, 1105 are rock shelters, and almost all occur in the Warton Sandstone formation (Kimberley Group: Lower Proterozoic), with some King Leopold sandstone sites near Kalumburu, in the northwest of the study area.

The Borologa rock shelter sites are isolated compact and indurated quartz sandstone (from here-on, 'quartzite') boulders of Warton Sandstone (Fig. 2). They are found at the base of a 20° slope that stretches from a series of stepped cliff-lines down to the northern bank of the Drysdale River (*marraran*, Kwini word for "river"). The Borologa sites lie at 90 m above sea level, the top of the adjacent plateau 230 m to the north reaching a further 239 m in height. At all elevations along the slope from the plateau to the Drysdale River, numerous large quartzite boulders can be found, most forming rock shelters containing rock art.

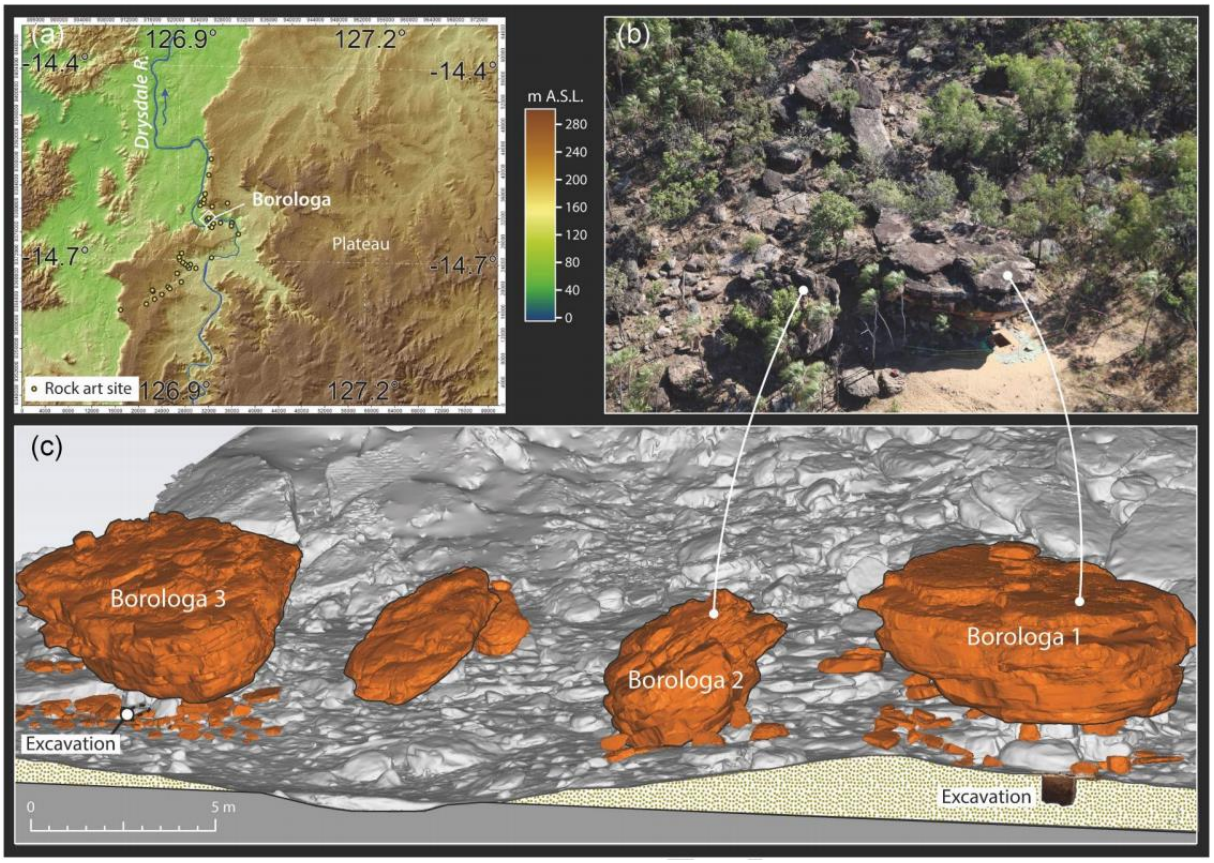

Figure 2. The Borologa sites, aligned at the base of the slope (photo and artworks by Jean-Jacques Delannoy and Kim Genuite).

Three of these rock shelter sites, Borologa 1–3, measure 15.5 m long × 12.2 m wide × 6.5 m high; 7.7 × 7.2 × 5.7 m, and 14.5 × 10.0 × 6.7 m respectively. Borologa 1 and 3 have been archaeologically excavated (David et al., 2019; Gunn et al., 2019). While buried archaeological evidence under their overhangs span more than 3000 years (bedrock was not reached due to massive roof-fall at c. 1.2 m depth), there is also above-ground and below-ground evidence in the form of artificially flaked, moved and stacked stone slabs that are primary evidence of people hollowing out alcoves, building walls and creating "site furniture" as far back as c. 9300 cal BP or more (for details, see David et al., 2019; Delannoy et al., 2020a). The variety and antiquity of the rock art styles present at Borologa 1 further suggests that people were painting there more than 11,500 cal BP (Finch et al., 2020), continuing into

the twentieth century CE. However, until now it has not been clear whether the Borologa rock shelters themselves have a deeper antiquity, or whether people first began to do things there as soon as the rock shelters had formed. Therefore, the question of how habitation within the sites, and the making of rock art, relate to regional occupational trends remains unknown. This has implications for our ability to determine regional demographic trends, socio-political divisions of the landscape, trends and patterns in engagements with places, and resource scheduling through time.

3 Geomorphological mapping

The Borologa 1–3 boulders are aligned above the Drysdale River's high-water mark, at the "front" (downslope end) of a boulder-strewn hill-slope (Fig. 2). The three boulders are of a similar size (see above for dimensions) and morphology to each other and less fragmented than those on the slope. The largest boulders all seem to have originated from escarpments higher up the slope, including some that now lie in the riverbed (Fig. 3). Unlike the large slanting blocks that dot the slope, the Borologa 1–3 boulders line up on the same topographic level perched 7 m above the river (Fig. 2). They are located beneath a cliff-line (E3 on Fig. 3c), near the bottom of the slope. The question remains as to their origins and antiquity, and of the geomorphological processes that caused their current morphologies and landscape setting.

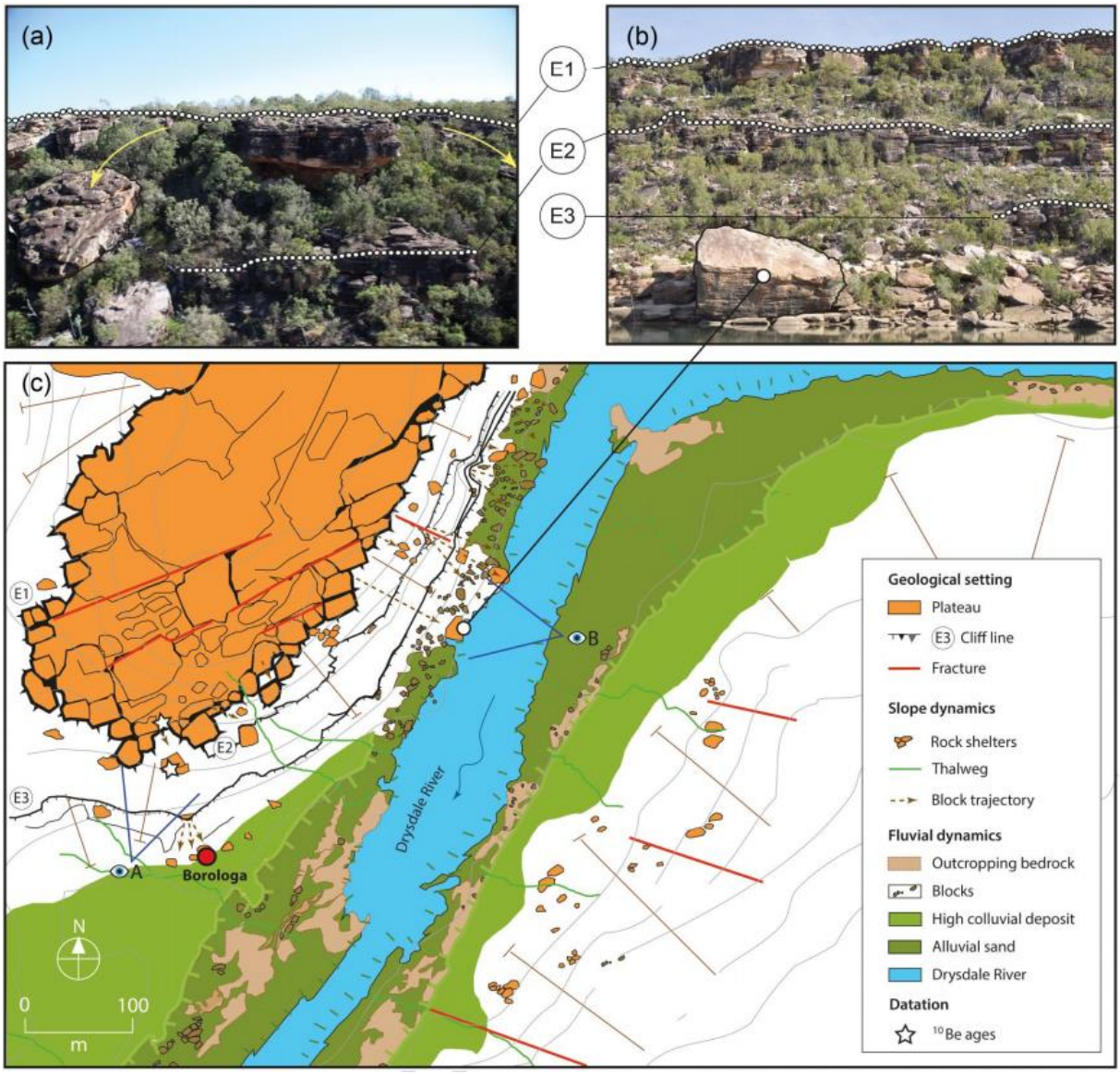

Figure 3. Location of Borologa 1–3 relative to the Warton Sandstone cliff-lines and associated slopes. Three cliff-lines can be identified. Borologa 1–3 sit below the lowermost escarpment, just above the Drysdale River channel. The white stars locate the two ^{10}Be cosmogenic profiles taken along vertical escarpment faces for exposure dating (photos and artwork by Jean-Jacques Delannoy and Kim Genuite).

4 Methods

To address how and when Borologa 1–3 formed, we undertook high-resolution three-dimensional (3D) mapping of the study area, along with geomorphological and

sedimentological investigations. Individual blocks along the slope below the lower cliff-line (E3 on Fig. 3), including those of Borologa 1–3, were digitally three-dimensionally conjoined to each other and to the cliff-line, their retro-fitting enabling reconstruction of the landscape before the arrival of people in the region more than 50,000 years ago (Veth et al., 2019; see also Clarkson et al., 2017), as determined from geomorphological reconstruction studies and cosmogenic exposure dating of vertical escarpment and matching detached block faces (the two white stars in Fig. 3).

To understand how sites such as Borologa 1–3 formed, it is important to consider the sites and their surrounding landscape at a nested range of spatial scales spanning from the cliffs near the top of the hill to the Drysdale River below. We began by constructing a Digital Elevation Model (DEM) from Shuttle Radar Topography Mission (SRTM) data, at a spatial resolution of 1 Arc-Second. Geomorphological mapping was also undertaken at a range of spatial scales, enabling the terrain's geomorphological history to be investigated. Given their archaeological interest, the Borologa 1–3 boulders were also 3D-mapped and geomorphologically investigated at higher spatial resolutions than the DEM model allowed (see Delannoy et al., 2020a).

4.1 3D mapping: scanning and data acquisition

The acquisition of topographic data and the construction of the ensuing 3D model aimed to digitally model the geometry of present-day blocks and their landscape setting (Kolbe et al., 2011). When coupled with data from a range of specialist research fields, 3D modelling becomes a powerful tool by which to investigate changes in terrain (Ballesteros et al., 2015; Campaña et al., 2016; Delannoy et al.; 2020b; Duvillard et al., 2018; Sadier et al. 2012). 3D modelling provides a topographic snapshot that can then be used to explore how the morphology and spatial relationships of objects have changed through time. This is done by

digitally establishing the current shape of surfaces and the position of objects relative to each other. Standard geomorphological techniques can add important details of diagnostic object properties, such as geochemical composition, mineralogy, height, morphology, colour, age and so forth (for results from Borologa 1, see Delannoy et al., in press).

The 3D model was constructed with a phase-shift Faro Focus 3D 360 Light Detection And Ranging (LiDAR) Terrestrial Laser Scanner (TLS). A five-step protocol for data acquisition was followed in the field: 1) the scanner was positioned to scan the area of interest for the research objective; 2) the scan window was defined; 3) the angle of the scan was chosen (this determines the density of the point cloud); 4) the scan was launched; 5) the scanner was repositioned along with an additional set of datum targets for the next acquisition (Jaillet et al., 2017) (Fig. 4). In our study, the LiDAR surveys were conducted at decimetric (2–10 cm) resolution for zones distant from the rock shelters, and centimetric to millimetric resolution within the rock shelters (Table 1). We conducted scans at 170 locations using spherical datum targets each measuring 14 cm in diameter. The quality of each scan's registration was evaluated by checking Cloud to Cloud matches through the mean value of 20 random measurements on the final 3D point cloud (Table 1). The registration of each scan, or "scene", was processed using *Faro Scene* and *CloudCompare* software (Girardeau, 2018). The final point cloud from which the 3D model was generated comprised more than 700 million points within an area of c. 5000 m^2 (Fig. 4).

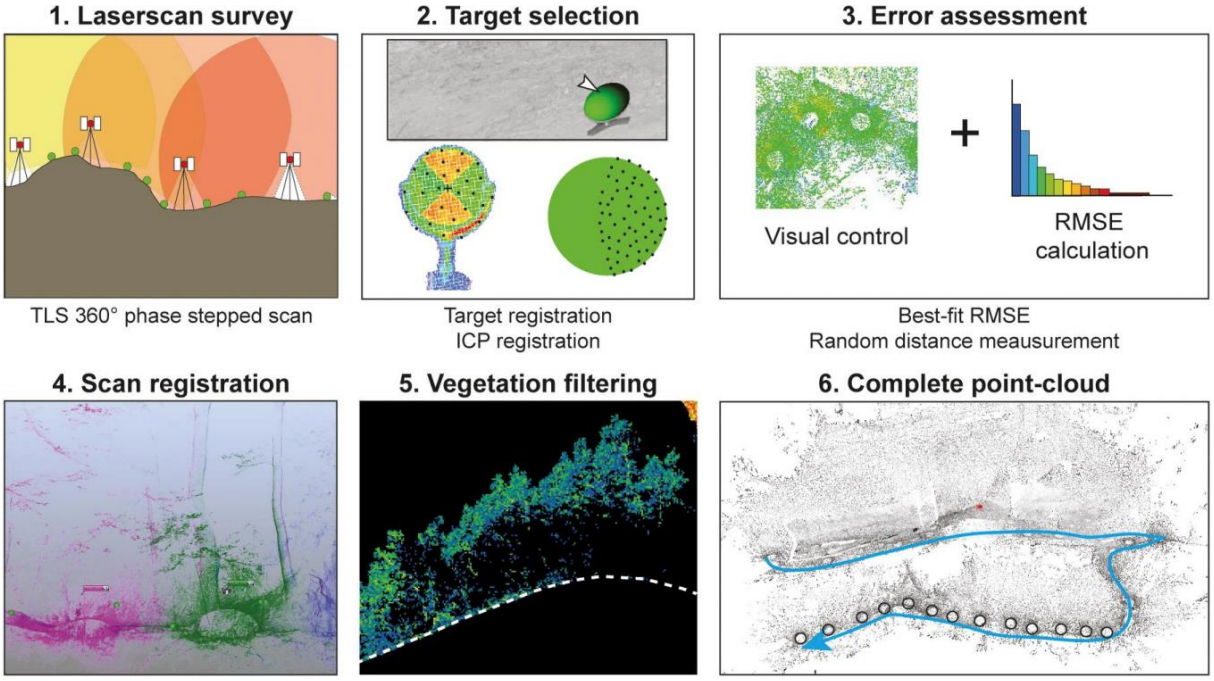

Figure 4. Workflow steps for TLS acquisition. All steps were processed by the same user (Kim Genuite) to minimise processing inconsistencies.

Table 1. Specifications of the 3D data acquired during the Borologa laserscan surveys (see also Delannoy et al., 2020a).

	Landscape setting
Survey method (A)	Short-range TLS + sphere registration
Point cloud accuracy (B)	1 cm
Point cloud density (C)	2 cm
Mesh accuracy (D)	2 cm
Mean size of Delaunay 3D triangles (E)	8 cm
Mapping tool (F)	Faro Focus 3D 360 (2012)
	Borologa 1–3 and nearby blocks
A	Short-range TLS + sphere registration

B	0.1 cm
C	0.6 cm
D	0.3 cm
E	1.2 cm
F	Faro Focus 3D 360 (2012)

	Excavation squares C5-C6-D5-D6-DV-DVI
A	TLS-constrained photogrammetry
B	0.1 cm
C	0.2 cm
F	NIKON D800 camera + 50 mm

4.2 Segmentation and meshing

Once a scan's data have been acquired by the software, the point cloud can be treated and cleaned of interfering items such as vegetation (e.g., Doneus et al., 2008; Lin & Zhang, 2014; Opitz & Nuninger, 2013; Sithole & Vosselman, 2005) (Fig. 4). For the Borologa sites, the 3D model was sliced into c. 100 cross-sections whose point clouds were manually cleaned to retain only the data points representing the ground surface and stone blocks (Douillard et al., 2011; Verhoeven, 2017).

The cleaned point cloud for each block or ground surface was then classified into object types. During field-based geomorphological mapping of the study area, some blocks had earlier been identified as sharing stratigraphic sequences or apparently matching surface morphologies with nearby larger blocks (boulders) or cliff-lines. These blocks were extracted from the complete point cloud and meshed separately. Only the blocks deemed to hold special significance (e.g., because they are flaked, or because they are important for understanding a boulder's geomorphological evolution) and those most comprehensively mapped during the

3D fieldwork were selected for separate meshing. The surface of each such object was modelled by Delaunay 3D linear triangulation with the *3DReshaper* meshing software (Delaunay, 1934; Gomes et al., 2009; Maur, 2002; Verhoeven, 2017) (Fig. 5). This method is the most suitable for visualising morphological changes in the relief and, in our case, the physical shape of archaeological landscapes (Verhoeven, 2017). Mesh refinement was conducted in several steps until the Delaunay 3D triangles for the cliff-line and blocks on the slope attained an average length of 8 cm (Remondino, 2003). Higher resolution triangles of average 1.2 cm length were used for the archaeological sections of the three main boulders (Table 1).

The boulders and other blocks deemed important to reconstruct the relief were individually meshed, so that they could be digitally moved to permit their retro-fitting one to another (Delannoy et al., 2020a). Accurate meshing was only possible for visible parts of each block. Buried parts were reconstructed on the basis of field observations, and the hard quartzite's regular angular morphology means that we can use the exposed surfaces to reasonably interpret the morphology of buried surfaces. Fracture patterns on exposed parts of blocks can also assist with the interpretation of the shape of their buried parts (Fig. 4). In the region around Borologa, quartzites of Warton Sandstone are compact and highly resistant to physical and chemical weathering, which means that significant irregularities in the fracture patterns are unlikely (physical impacts notwithstanding) (Cazes et al., 2020), as evident also by the frequent accurate conjoining of block surfaces and of detached blocks and their originating escarpment (see below).

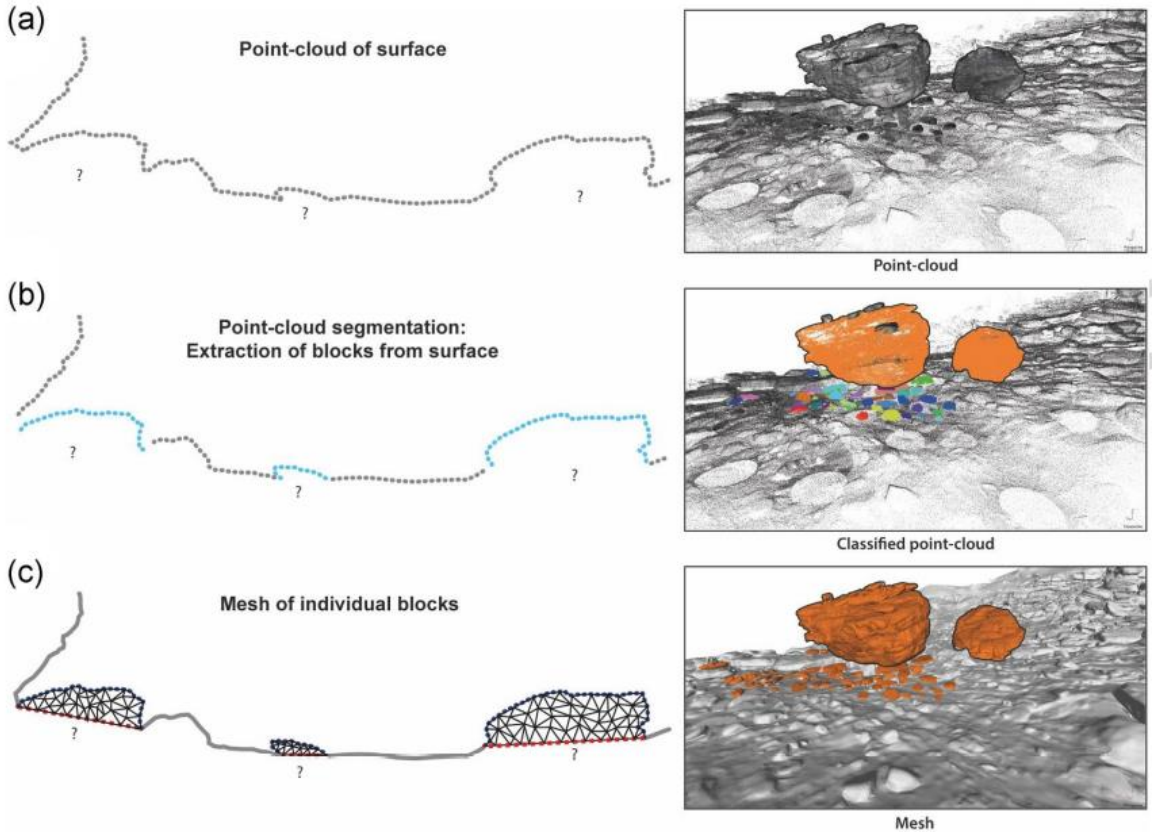

Figure 5. Meshing of individual blocks. Left-hand column: A: the full surface of the scanned landscape, as determined by the point cloud from the LiDAR scans. B: the point cloud has been segmented to separate out individual blocks. C: each block has been individually meshed. Right-hand column: the same steps as the left-hand column are shown for a large part of the Borologa slope (artwork by Kim Genuite).

4.3 Stratigraphic correlations and measurements

The characteristics and thickness measurements of strata recorded in the field for Borologa 1–3 and nearby blocks (David et al., 2019) enabled us to validate the measurements acquired from the 3D model. Close correspondence between the field measurements and those obtained digitally from the 3D model give confidence to the latter's accuracy, even for highly complex or more difficult to reach parts of the landscape such as elevated cliffs. In the 3D model, thickness measurements were taken between selected points along the top and bottom of each

stratum (Fig. 6). The two reference points were selected at right angles to the mean orientation of the rock face, which was obtained by fitting a planar mesh on the rock face of cliffs and large blocks, and along strata planes of smaller blocks. Like matching bar codes, this first step of investigation allowed us to match the stratigraphic sequences of paired blocks and outcropping bedrock (including cliffs) (Fig. 7). In no case were voids present between a studied block and its potentially conjoining bedrock; the interface between two adjacent rock masses did not show any roughness or empty spaces between them (as could be expected from detachments of rock slabs by impact if blocks had tumbled down the slope). This is further support that the studied blocks slowly slid down rather than tumbled down the slope following detachment (see below).

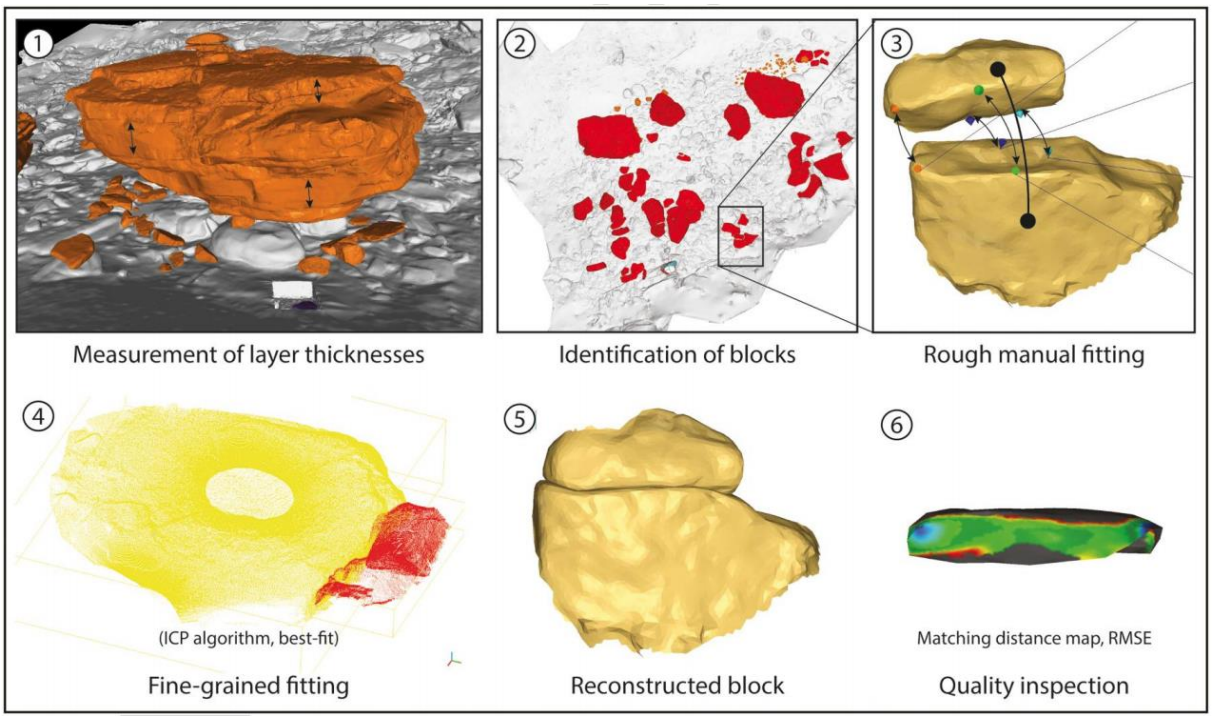

Figure 6. Retro-fitting techniques used in this study. Even when the strata and morphology of blocks appear to match, successful conjoining is not always possible. Various tests (including field observations) were used to interrogate each conjoin set. A matching distance map (bottom right-hand image) is a visual representation of the distances between two objects

measured in 3D. It can be performed between point clouds, meshes or both on 3D software such as CloudCompare M3C2 plugin (James et al., 2017) or 3DReshaper inspect tool (Carraro et al., 2019). Such matching distance maps can be compared to root mean square error (RMSE) measures that help check the quality of fit between surfaces. Poor matches can be caused by non-conjoining blocks, insufficient mesh accuracy, impeded readings (masked areas), or erosion of surface areas (artwork by Kim Genuite).

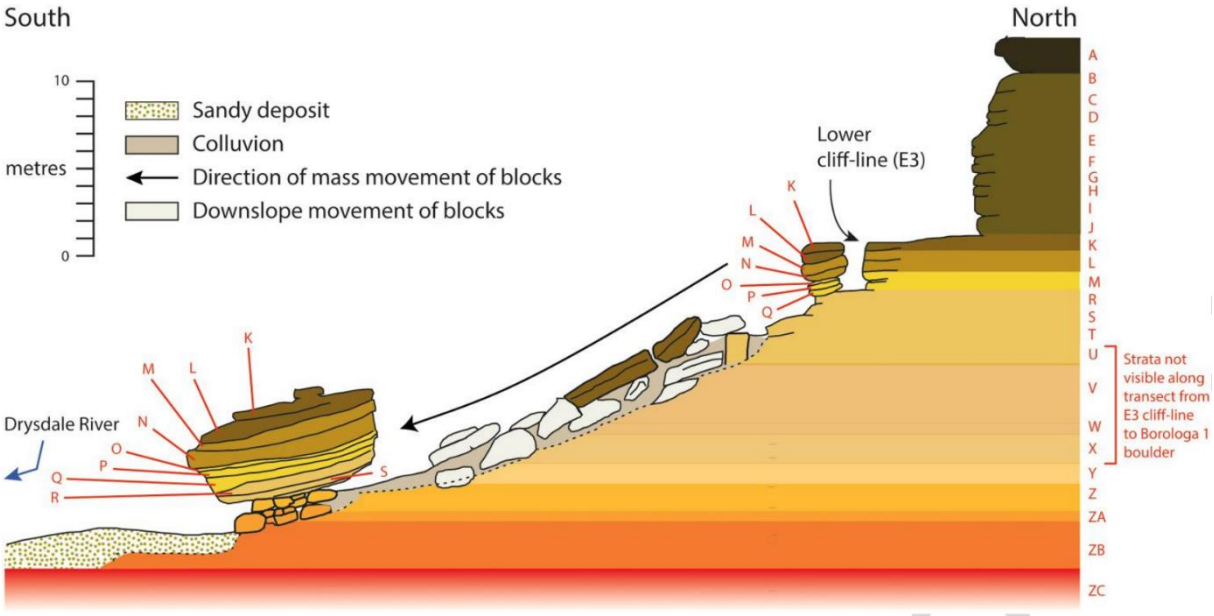

Figure 7. Stratigraphic sequences of the Borologa 1–3 boulders and Warton Sandstone lower cliff-line (E3). Strata U to X are not visible along the slope between the lower cliff-line (E3) and the Borologa 1 boulder, because they are obscured by loose surface deposits. They are nevertheless visible to the side of this transect, where they are exposed along shallow gullies. Strata thicknesses were measured from the 3D model (artwork by Kim Genuite).

To facilitate visualisation, we have colour-coded the individual rock strata on each block and on the lower cliff-line (E3 on Fig. 3; see Figs 7, 9; Appendix A). These identifications began with the characterisation of the 29 discrete strata that make up the Borologa 1 boulder

(Fig. 7), as determined by their individual thicknesses, texture, grain size and compaction (for details, see Delannoy et al., in press).

4.4 Geomorphological observations

A two-dimensional (2D) topographic shadow map was also generated for the study area (Fig. 8). Morphometric and surface hydrological analyses were conducted on the 2D raster elevation model and from field observations. The 2D raster map was processed from resampled 3D Delaunay triangles, to benefit from the smoothing provided by the Delaunay 3D meshing process (Ilic, 2005; Remondino & Campana, 2014). The sampled point cloud was rasterized using *CloudCompare* software (Girardeau, 2018; Verhoeven, 2017) at 2 cm resolution across the study area. The hydrographic network modelling was performed with *GRASS GIS* software and the *r.flow* module (Mitášová & Hofierka, 1993).

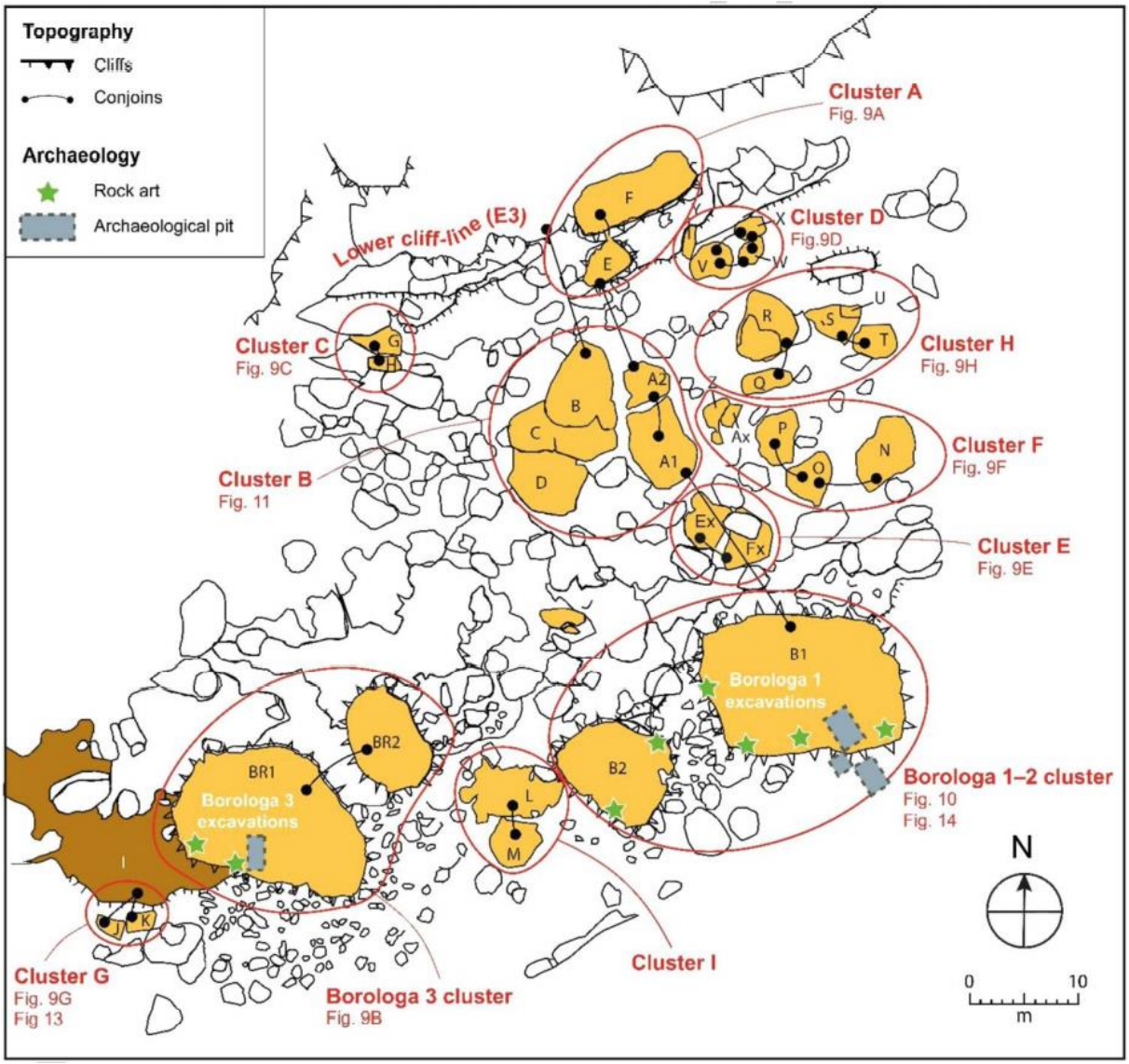

Figure 8. Map of conjoining blocks (orange) and bedrock (brown) between Borologa 1–3 and the Warton Sandstone lower cliff-line (E3) further upslope. The conjoining blocks were determined by matching rock strata sequences and surface morphologies (artwork by Kim Genuite).

4.5 3D retro-modelling

Having characterised the individual rock strata constituting the quartzite blocks, we investigated whether the blocks had eroded from the cliff-lines higher up the slope. We began by attempting first to digitally conjoin individual blocks to each other, and then to the cliffs.

This process was fulfilled in two steps (Fig 6). First, we attempted manually to refit digital models of blocks using a point-paired alignment process. Blocks were selected for refitting based on visual assessments of their morphologies (i.e., their apparently matching features were manually checked for how well they conjoined). The successful conjoin sets were then confirmed through an iterative closest-point (ICP) best-fit algorithm (Besl & McKay, 1992), which minimises 3D distances between object surfaces by directly matching portions of two-point clouds (Sharp et al., 2002; Shi et al., 2006). Refitting through ICP was conducted using *3DReshaper* and *CloudCompare* software (Girardeau, 2018). Reconstructions were first conducted for clusters of spatially proximal blocks and then spread out further afield, as the likelihood of finding conjoining blocks increased with proximity. The cluster identifications were based on field observations (interlocking morphologies of the block surfaces), in the field working upslope to their originating escarpment. Subsequent 3D modelling of the blocks confirmed and refined the association of the blocks within each cluster, and from cluster to cluster. The root mean square error (RMSE) values issued from the ICP algorithm is a measure of the confidence level for the conjoin set (Sharp et al., 2002). When RMSE data are not available – for example, when conjoins are conducted visually or when the point cloud data are unreliable for refitting purposes, such as for highly weathered surfaces – other observation-based criteria are required to assess the quality of reconstructions.

When attempting to reconstruct and assess correlations between matching blocks using these methods, the best-fit and RMSE method may not always deliver satisfying results and can thus be difficult to interpret, even for blocks which evidently fit together. The results of the RMSE method may thus vary according to the quantity of points selected for best-fit calculations and the topography of the surfaces adjacent to the selected points (Appendix A). Various factors affect the accuracy and precision of the best-fit method, including the variable weathering of surfaces and fracture lines; incomplete measurement data (e.g., due to the burial

of some surfaces); and low scan and mesh resolution. For this reason, the reconstructions also rely on field measurements and observations of rock strata and surface morphologies that can be used as controls for cross-checking the quality of individual reconstructions (Appendix A). Where field data are available, in instances where best-fit matches cannot be obtained, stratigraphic correlations based on visual inspections, petrographic characterisations and measurements of strata thicknesses can sometimes be made. By 3D retro-fitting the larger and better-preserved blocks, we can thus gain new insights into the sequencing, processes and (relative) chronologies by which sites and landscapes have changed through time.

5 Results

5.1 Stratigraphic correlations

The reconstructions of closely-matching stratigraphies between adjacent and widely-spaced blocks show that many were once joined, either as spatially widespread multi-layered conjoin sets, or closer to the remnant cliff-line. Subsequently we investigated whether these conjoin sets (including the Borologa 1–3 boulders) were once part of the now-receded Warton Sandstone lower cliff-line (E3 on Fig. 7), having gradually moved downslope to their current positions. We observed that the stratigraphy of each of the large blocks does not correlate with that of the bedrock that outcrops near ground level, lower down the hill. Rather, blocks with rock strata U to X occur as isolated pieces between the cliff-line and the base of the slope (Fig. 7).

In Figure 8, we have allocated letters to individual blocks, and cluster names to conjoin sets. The stratigraphic sequence of Block E (in Cluster A), a rock stack up to 5.7 m tall represented by seven distinct strata, could be both matched and conjoined with that of the outcropping lower cliff (E3) 1 m to the north (Fig. 9A). Across the study area, the tower-like

blocks have only been displaced from their conjoining cliff faces by short distances, and never exceed 1 m.

Blocks located near the western part of the lower cliff-line (Cluster C, consisting of Blocks G and H) are all composed of strata R–T. Here a lateral surface of each block could also be digitally conjoined with a high degree of confidence (Fig. 9C; Appendix A). The eastern part of that same cliff-line, where Cluster D (Blocks V–Y) is located, is especially interesting because the ground surface consists of outcropping bedrock (Fig. 9D). Some of Cluster D's blocks, again composed of strata R–T, have detached from the lower cliff and slid down a few decimetres only. Block Y (measuring 2.5 × 0.6 × 0.5 m) from Cluster D is found against Block V (Appendix A). It belongs to stratum Q, which means that it is some 1.6 m from its source location.

Cluster E comprises two conjoining parts (Blocks Ex and Fx) of what was once a large tabular block (Fig. 9E). The two blocks are 0.8 m apart. Among Cluster F (Blocks N–P), the matching of strata sequences between blocks was more challenging, because many of the blocks were partially buried (Fig. 9F). While all the blocks appeared to have originated from strata K and L, we were unable to acquire consistently reliable thickness measurements to confirm this. Nevertheless, closely matching fracture morphologies enabled accurate conjoin sets to be assembled (e.g., Blocks Z and Ax).

Reliable inter-block correlations were established for the lower western and southern parts of the study area (including Borologa 1–3 and adjacent blocks), where large low-lying bedrock surfaces outcrop (Fig. 9G). The Cluster G blocks (J–K), both of which, along with outcropping bedrock I, could be refitted to each other through a combination of matching strata and conjoining surfaces, had been separated through tilting and fracturing. Tilting matching with slope angles had affected all the conjoining blocks, but none were found up-side down (see Discussion below).

Cluster H (Blocks Q–U) is located between the lower cliff-line (E3) and Borologa 1–3, on outcropping bedrock on the eastern side of the study area. Here the blocks and bedrock are partially buried. The blocks all have similar tabular morphologies, which suggests that they all came from a single rock stratum. This rock stratum is visible in the field in the E3 escarpment, where Blocks Q–U originated.

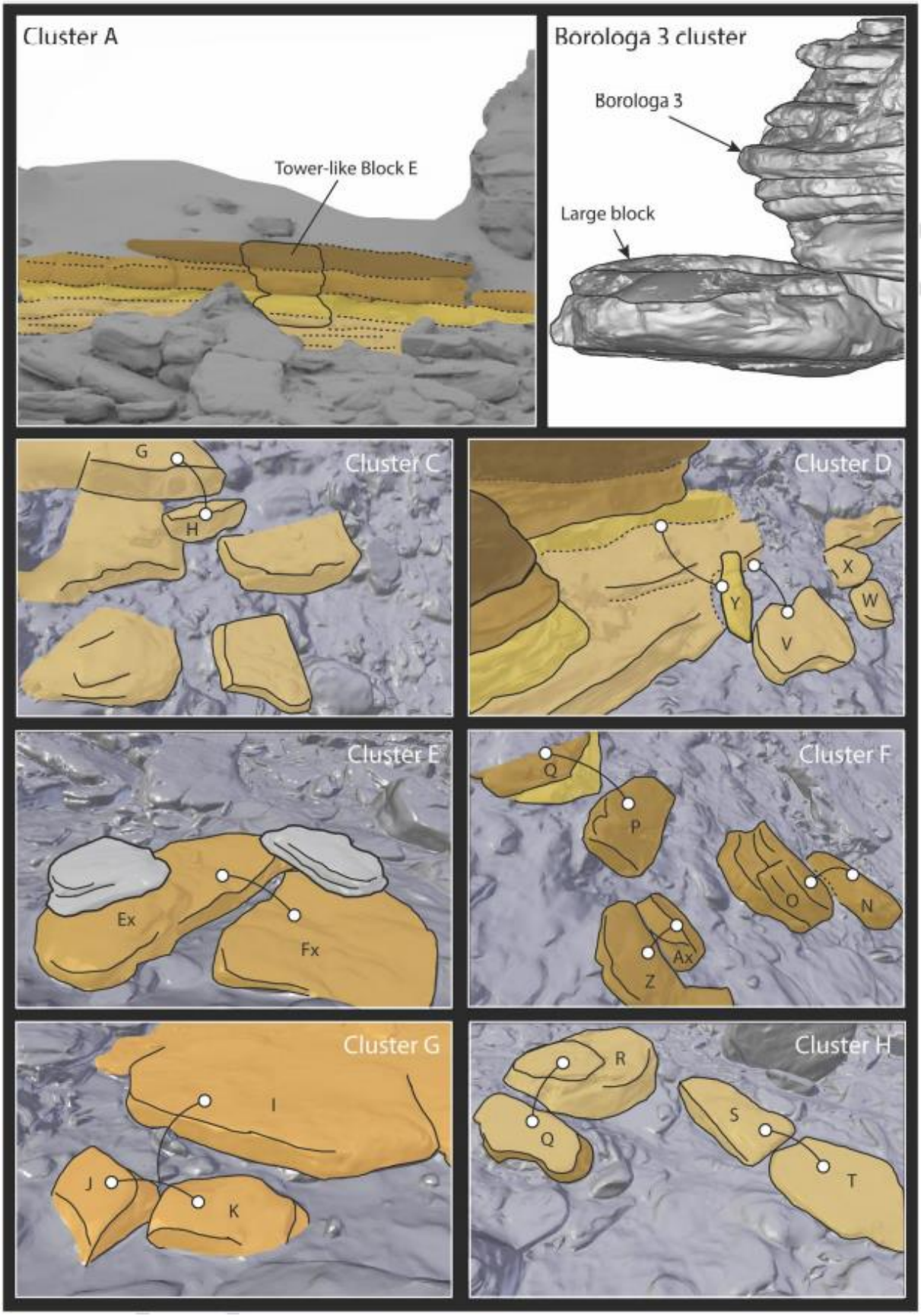
Cluster A
Tower-like Block E
Borologa 3 cluster
Borologa 3
Large block
Cluster C
G
H
Cluster D
X
Y
W
V
Cluster E
Ex
Fx
Cluster F
Q
P
O
N
Ax
Z
Cluster G
I
J
K
Cluster H
R
Q
S
T

Figure 9. Matching blocks by cluster group (see Fig. 8). The conjoining blocks are represented by white dots; the corresponding rock strata are colour-coded (see Fig. 7) (artwork by Kim Genuite).

5.2 Borologa 1–3

Matching stratigraphic sequences and surface morphologies allowed Borologa 1 and 2 (Blocks B1 and B2) to be conjoined, indicating that together they once formed a large rock shelter with a long overhang. The two large blocks were re-assembled with excellent RMSE correspondence (Appendix A) and matching rock strata sequences (Fig. 10), although noticeable cavities are evident in strata U–X of both (Figs 7, 10B), suggesting that those strata may have been more sensitive to weathering than the upper ones (Wray, 1997).

The stratigraphic sequences of Borologa 3 (Block BR1) and Block BR2, 4.3 m away, correspond well, as do their surface morphologies, forming a secure conjoin set. Although the digital best-fit values suggest that the blocks conjoin well, here again the two parts have occasional gaps between their matching surfaces (note that no attempt was made to digitally conjoin small blocks that may fill these gaps).

The stratigraphic sequences of the Borologa 1–2 and Borologa 3–BR2 conjoin sets match well, indicating that they came from a common source, even though today the two clusters are some distance apart (Figs 2, 9B).

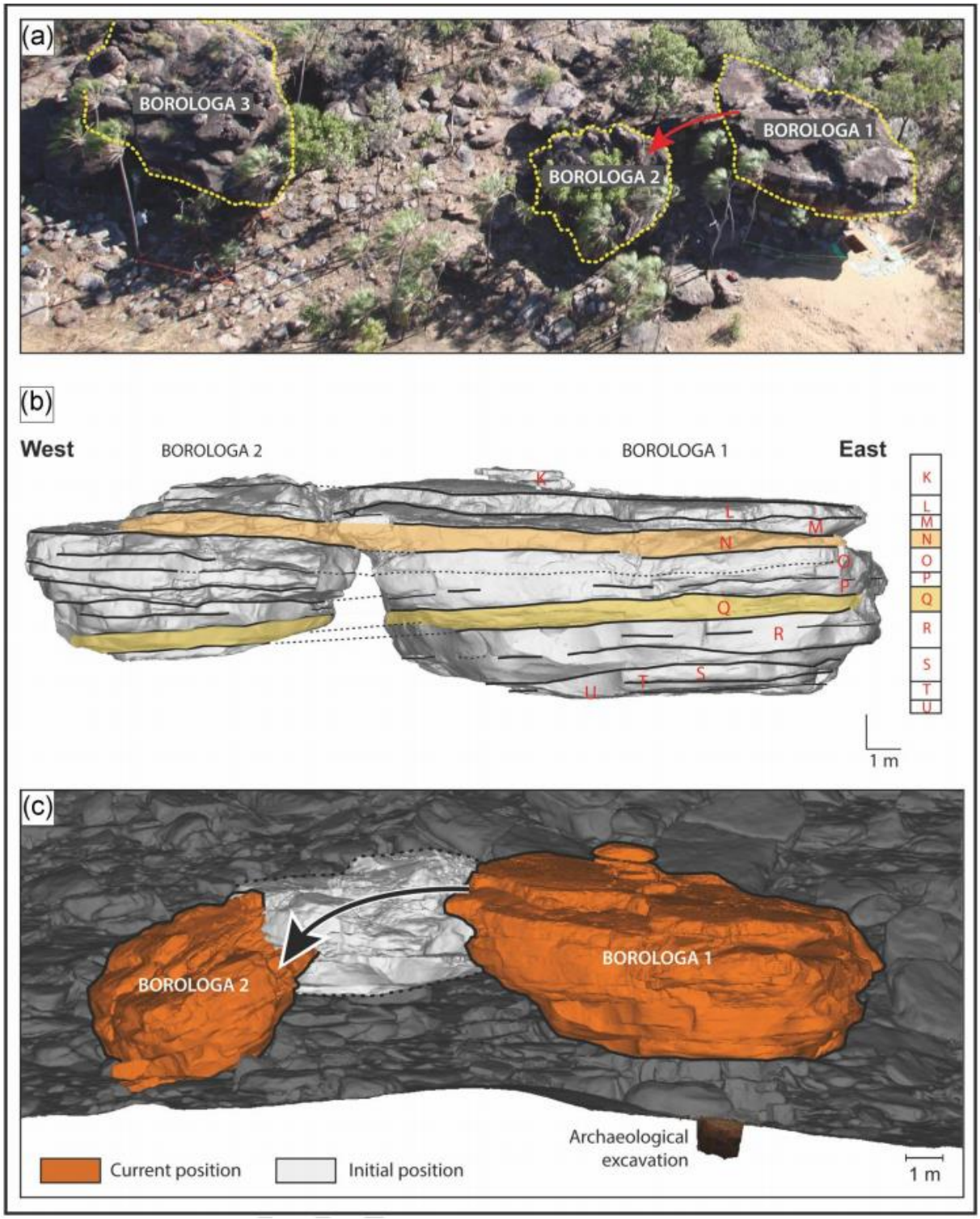

Figure 10. Borologa 1 and 2 (Blocks B1 and B2). The 3D reconstruction was processed by ICP correlation, and displays a high level of stratigraphic coherence (artwork by Kim Genuite).

5.3 Rock shelters and the Warton Sandstone lower cliff-line

We attempted to re-position the Borologa 1–3 conjoin sets to their originating positions along the lower cliff-line near the top of the slope. Blocks that had corresponding strata K–U thicknesses and morphologically matching surfaces could be merged to construct a tabular conjoin set that could be refitted onto the cliff (Fig. 14). The matching strata were consistent with their conjoining edge morphologies, a good indication of the reliability of strata correspondences among the hard and slow-weathering quartzites of the Warton Sandstone formation (Cazes et al., 2020; Delannoy et al., 2013) (Fig. 3). Conversely, many blocks could not be matched, often because vegetation or sediments covered important details relating to the thickness of individual strata and surface morphologies. Not all blocks could thus necessarily be conjoined back to other blocks or to their originating cliff-lines. The final 3D reconstruction is therefore spatially incomplete, even where the strata of many blocks are known.

5.4 Geomorphological mapping

Many of the blocks investigated in this study appear to have progressively slipped downslope from the lower cliff-line. None were found upturned. All the studied blocks along the slope are in a normal stratigraphic position, their displacement along the slope being mostly across short distances. All the field and mapping evidence indicates that none of the studied blocks have tumbled down the slope. Blocks originating from given strata are nevertheless sometimes dispersed, indicating for those cases wide-spread movements down the slope. Less can be said of the west side of the study area, because of a paucity of topographic data relating to the slope and its cliff-line higher up. The down-hill (colluvial) transport of blocks largely ended on an exposed, flat, sub-horizontal bedrock surface near the base of the slope that is today partly covered by both alluvial and aeolian sands.

The hydrographic network computed from the DEM model divides the hill-slope into two main micro-catchments. One of these micro-catchments flows to the east of Borologa 3, in the process eroding out stratum Zc, the partially buried bedrock (Fig. 7). In the other micro-catchment, water flows to the east of Borologa 1. The archaeological deposits of Borologa 1 and Borologa 3 are found in relatively well-protected areas away from these drainage pathways (David et al., 2019); i.e., buried cultural deposits are better preserved in these locations than where slope-wash is more prevalent (Fig. 11).

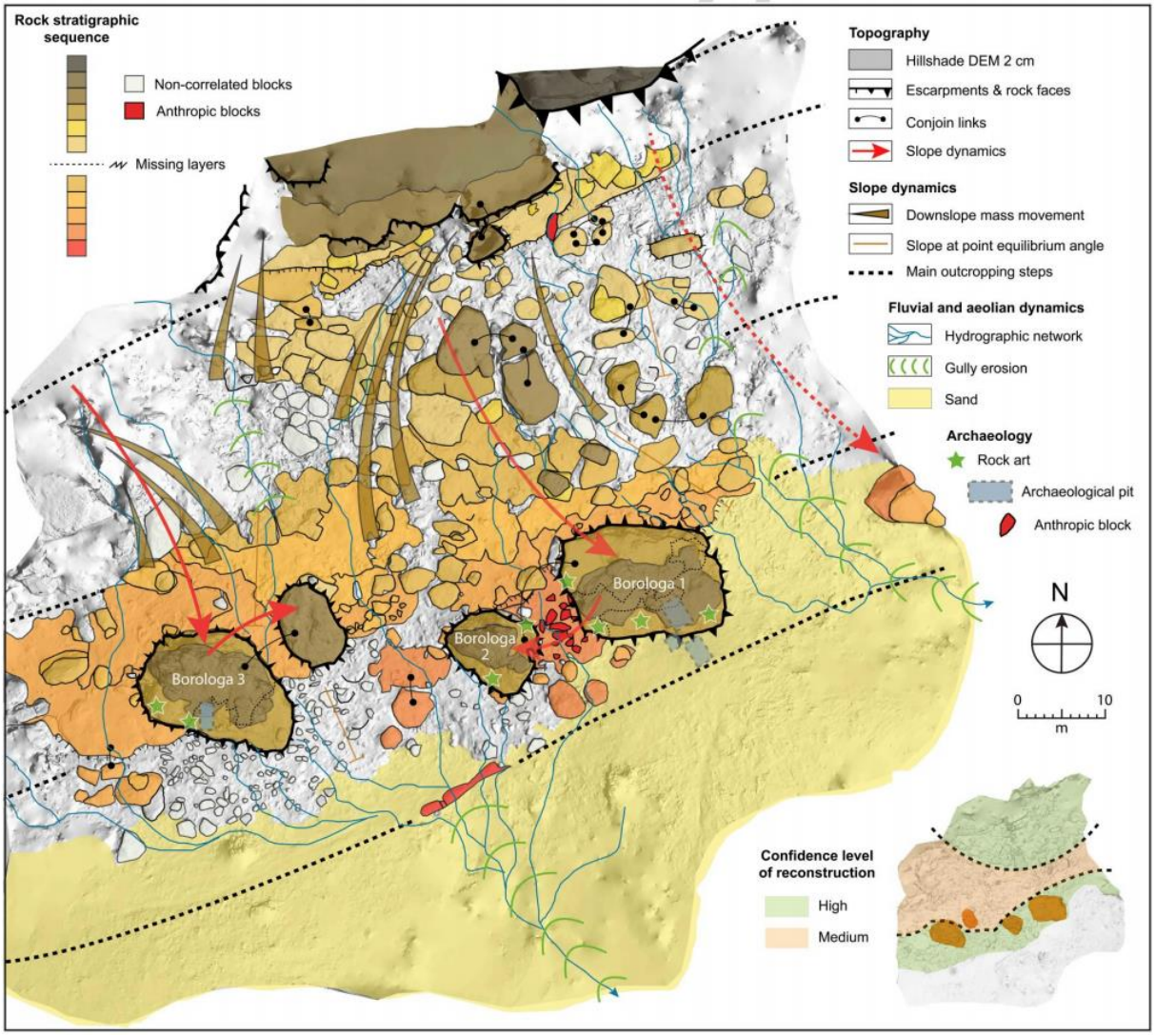

Figure 11. Interpretative map of the rock strata exposed along the Warton Sandstone low cliff-line (E3) and downslope blocks. Note that the level of confidence decreases with distance

from the cliff-line, except for near the base of the hill where the bedrock again outcrops (artwork by Kim Genuite).

The geomorphological study at high spatial resolution made it possible to detect the presence of slow water action between the large blocks on the slope and bedrock. This is very clear at Borologa 3, where a finely laminated mineral accretion (cement derived from dissolution and reprecipitation) occurs between the base of the boulder and its pedestal, just north of the archaeological excavation squares (bedrock) (Fig. 12). X-ray diffraction (XRD) analysis on the accretion identifies it consisting of 13.5% calcium oxalate (whewellite, $CaC_2O_4 \cdot H_2O$), 4.1% calcium sulphate (gypsum, $CaSO_4 \cdot 2H_2O$) and 82.5% quartz, with the latter likely to largely reflect the inclusion of quartzite bedrock material on the underside of the analysed accretion. The accretion's presence indicates processes of dissolution and reprecipitation of constituents of the sandstone. A radiocarbon age on the calcium oxalate minerals in the outer lamina of the accretion gave an age of 7177–7426 cal BP (6385 ± 62 BP (OZW427U1), calibrated with IntCal13 at 95% probability). The formation of the accretion between the bedrock and Borologa 3 indicates that Borologa 3 was already in place by the start of the Middle Holocene, and Block BR2 had already separated from it.

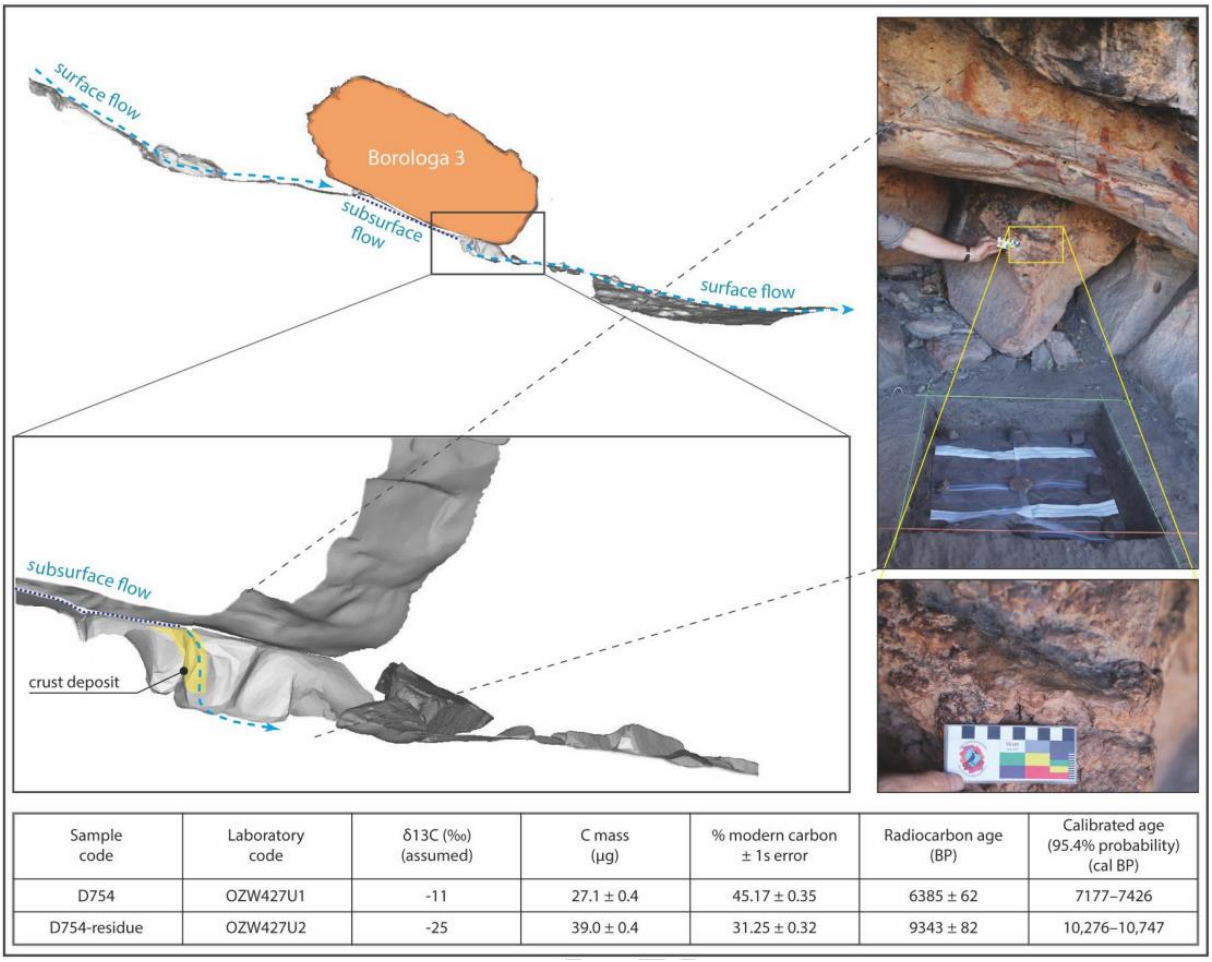

Sample code	Laboratory code	δ13C (‰) (assumed)	C mass (µg)	% modern carbon ± 1s error	Radiocarbon age (BP)	Calibrated age (95.4% probability) (cal BP)
D754	OZW427U1	-11	27.1 ± 0.4	45.17 ± 0.35	6385 ± 62	7177–7426
D754-residue	OZW427U2	-25	39.0 ± 0.4	31.25 ± 0.32	9343 ± 82	10,276–10,747

Figure 12. Radiocarbon-dated mineral crust on quartzite block on Borologa 3 floor, near the archaeological excavation pit. Calibrations undertaken in Calib 7.10 with IntCal13 curve selection (Bronk Ramsey, 1995; Reimer et al., 2013). Top left: longitudinal section down the slope. Downslope waterflow passes between the boulder and the bedrock. Bottom left: close-up view of the junction between the boulder and the bedrock, where a sample of the accretion was taken for radiocarbon dating. Top right: photo of the accretion in place (before sampling). Bottom right: close-up view of the radiocarbon-dated accretion (photos by Jean-Jacques Delannoy).

Geomorphological investigations along the upper slopes above Borologa indicate that large masses of quartzite have also detached from the upper escarpments (E1 and E2 on Fig. 3). Preliminary modelling of ^{10}Be cosmogenic nuclide profiles along vertical exposed faces

suggest that the displacement of these massive quartzite boulders from the upper escarpments E1 and E2 rock surfaces occurred more than a few hundred thousand years ago, indicating the overall relative stability and antiquity of the landscape as observed today (the quantitative data for the cosmogenic-derived exposure ages will be published elsewhere).

6 Discussion

Coupling 3D retro-modelling methods with geomorphological mapping yields important details of palaeo-slope movements that enable improved understandings of how individual blocks (some with significant overhangs) came to be where they are now. This enables us to better situate accumulated archaeological deposits in their broader landscape settings. While a paucity of corresponding rock strata and matching boulder-edge morphologies means we cannot determine exactly where Borologa 3 and its conjoining Block BR2 came from, Borologa 1 and 2 can conclusively be shown to have originated from the Warton Sandstone's lower cliff-line, as determined by both matching strata and conjoining rock surface morphologies (Fig. 3; Appendix A). Furthermore, the oldest detached blocks from cliff-line E3 (including Borologa 1–3 and BR2) are now located at the bottom of the slope (we know this because of the sequence of detachments, as determined by the retro-fitted blocks and cliff-line). The presence of gullies emanating from the cliff-line confirms the existence of preferential downslope pathways to the base of the hill (Fig. 11). Most of the large blocks with archaeological deposits and rock art are not locally outcropping rock stacks, but rather blocks detached from cliff-lines up the slope, and in some cases redeposited directly on top of rock pavements. Given that large blocks usually detach and collapse from cliff-lines in sets as mass movements rather than gradually as isolated blocks (e.g., Bachmann et al., 2009; De Vita et al., 2013), the downslope migration of the Borologa blocks from the escarpment almost certainly took place gradually over long time-frames, which, based on cosmogenic

^{10}Be exposure dating in the order of c. 100,000 years, ceased when the largest blocks (Borologa 1+2 and Borologa 3) reached their present alignment at the base of the slope. The implication of such a coordinated process of detachment and downslope migration is that, across the landscape, boulder formation was punctuated. New habitable sheltered spaces were thus likely to have become available in staggered time-scales across the landscape, and this could have significance for understanding patterns of site and regional occupation as determined by the archaeology of deposits and rock art. This emphasises the importance of determining when, and how, rock shelters formed when determining occupational trends within sites and across landscapes. Such questions also lead us to further examine the mechanisms of landscape evolution for the Borologa hill-side (see also Cazes et al., 2020; Young, 1987).

6.1 Tilting

The tilting of large standing quartzite blocks is clearly revealed by the retro-modelling (Fig. 13). Vertical fractures from mechanical stress along the cliff-lines caused large blocks to detach through the effects of gravity along topographic gradients (Fig. 11). Tilted detached blocks are seen almost everywhere in the study area, indicating that they have slid down from higher levels. One of the most striking of these is Borologa 2, which collapsed from its parent body (Borologa 1) by tilting at an angle of 30° towards the west (Fig. 10).

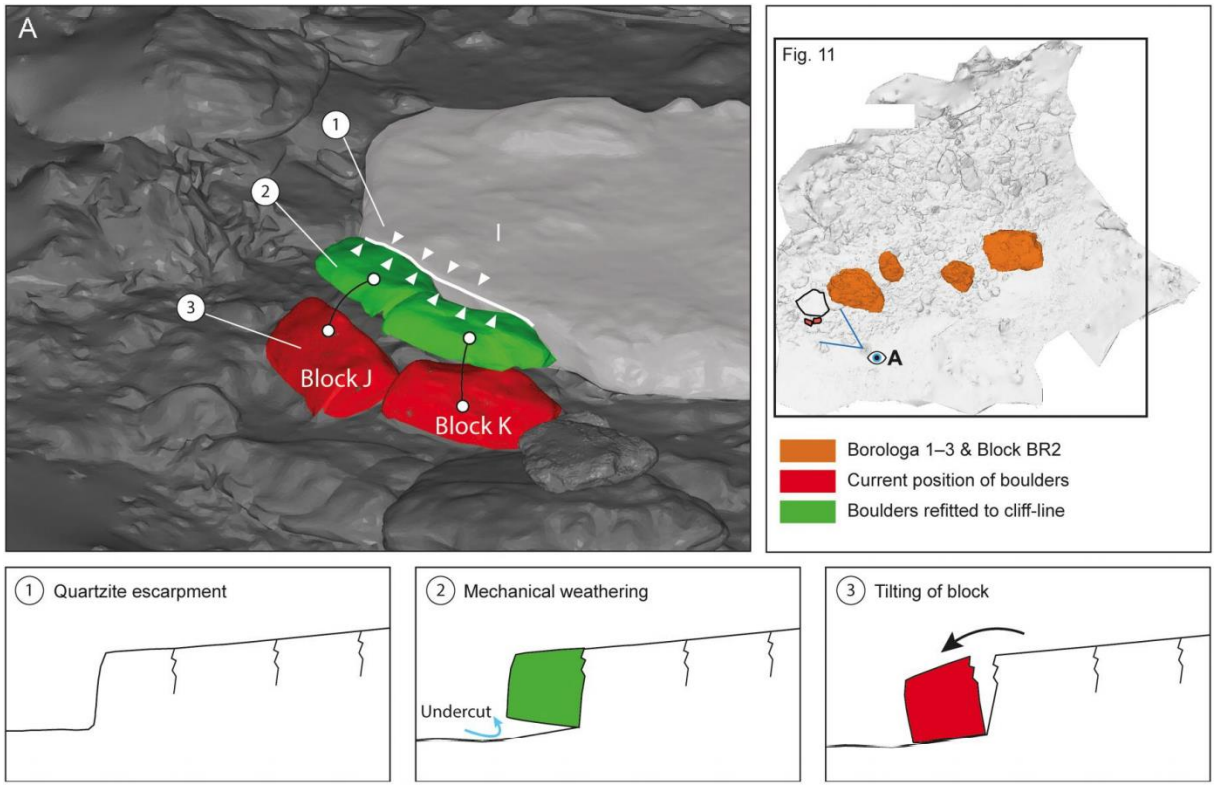

Figure 13. Tilting process for Blocks J–K from exposed bedrock I (see Fig. 8 for precise locations). The blocks did not reptate far down-slope (artwork by Kim Genuite).

6.2 Sliding

The 3D conjoin sets allowed the repositioning of some blocks higher on the hill than where they currently sit. Unlike some of the larger, upslope blocks (Fig. 3), the Borologa 1–2 and Borologa 3–BR2 conjoin sets reveal minor changes in their orientations relative to their original positions: the blocks tilted and slightly rotated as they moved downslope (Figs 13, 14). Nevertheless, the general retainment of their prior orientations was likely due to their slow reptation (snake-like slithering movement) down the slope. The slight shifts in orientation appear mainly in conjoined Borologa 1–2, which was inclined 20° as it slid more or less parallel to the slope.

The question remains as to when in the past the blocks became detached from the cliff-line, prior to sliding downslope to their current positions. Cosmogenic ^{10}Be nuclide measurements

from the Drysdale River catchment provide critical insights on cliff-line denudation rates (Cazes et al., 2016, 2020).

The slope gradient on which the Borologa sites sit is at a limit equilibrium angle of 20–25º (e.g., Brunsden, 1999; Crozier, 2010; Delannoy et al., 2016), indicating that the blocks are unlikely to further slide through gravity under current conditions. The fact that the boulders largely preserved their original orientations as they slid down the slope (the "translation" process) indicates very slow movements. Further up the slope, preliminary ^{10}Be cosmogenic nuclide exposure ages of vertical cliff faces suggest that the detachment of large boulders from escarpments E1 and E2 (see the white stars on Fig. 3C) occurred no earlier than a few hundreds of thousands of years ago, and perhaps half a million years ago (these data will be published elsewhere). Our results indicate a very slowly evolving landscape, mainly through lithologically-controlled topographic features, gravitational processes and slope dynamics (Cazes et al., 2020).

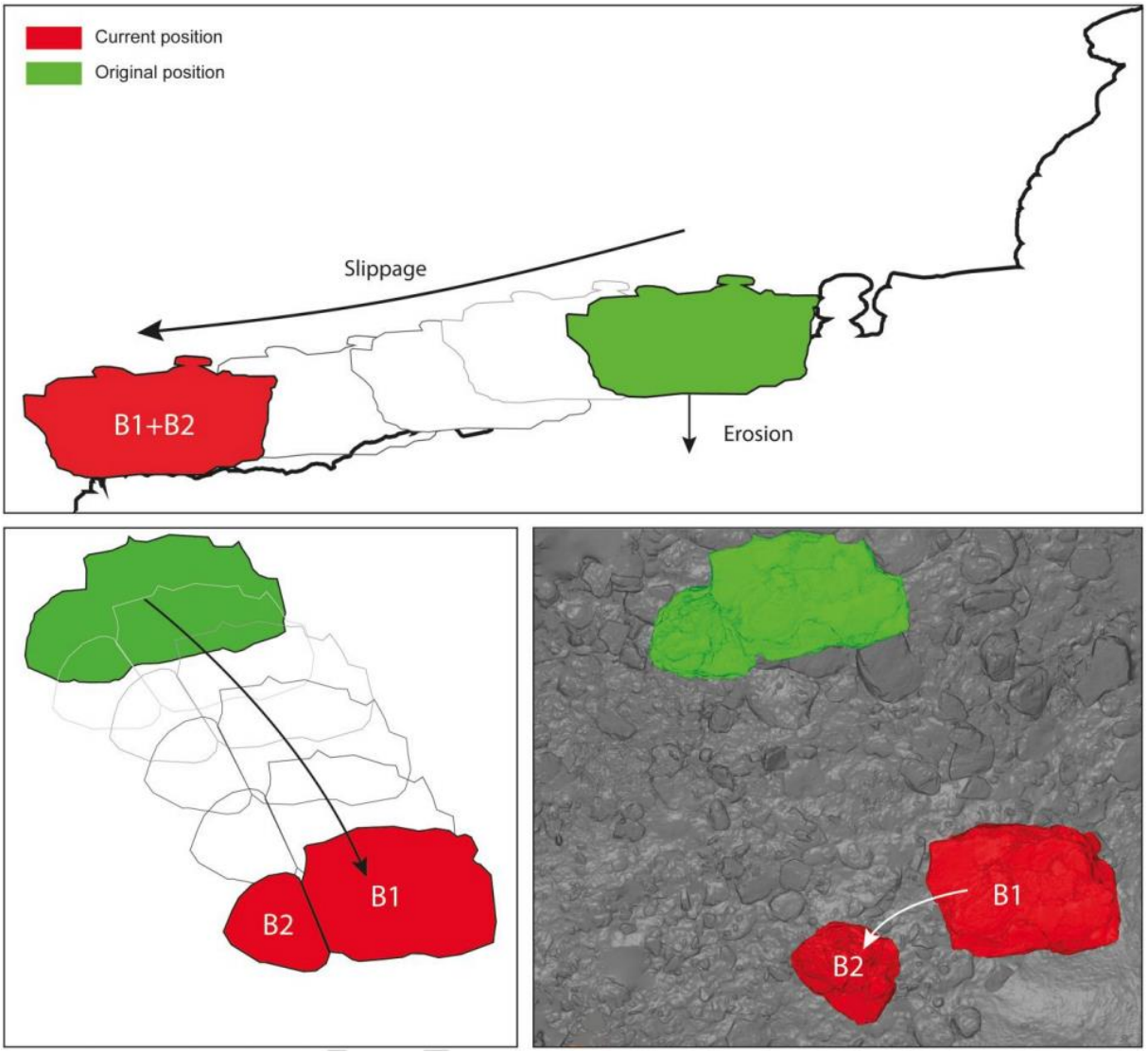

Figure 14. Sliding processes that affected the Borologa 1–2 boulder complex (artwork by Kim Genuite).

7 Conclusion

Increasingly, research across the world has shown that what had previously been presumed to be "natural" caves and rock shelters had in fact been modified through the actions of people (e.g., David et al., 2017, 2019; Delannoy et al., 2017, 2020a; Jaubert et al., 2016). But to determine exactly how people had modified the material fabric of a site, and the significance of those modifications for subsequent activities, we must first ascertain what the site was like prior to its human-induced modifications. Establishing the lay of the land before and after first

occupation is also important for a proper evaluation of landscape processes. By coupling field-based geomorphological investigations with digital 3D conjoining of displaced quartzite blocks along the slopes of Borologa onto cliff-lines, the landscape's morphogenic history can be determined over a long, geological timescale (Fig. 15). The methods presented in this paper are particularly applicable to hard, compact geological formations subject to slow weathering, where conjoining rock surfaces will have better preserved over long periods of time.

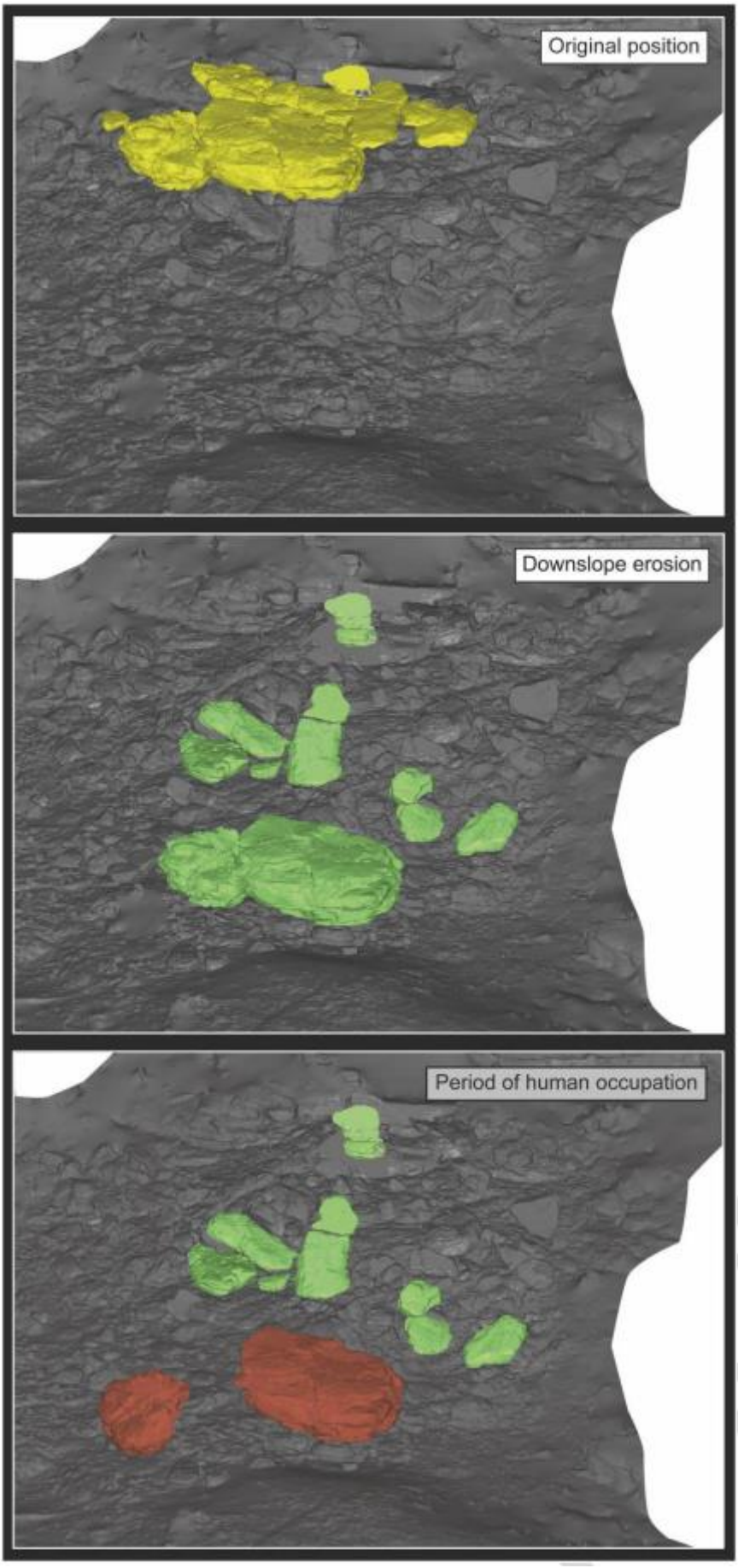
Original position
Downslope erosion
Period of human occupation

Figure 15. Evolution of the Borologa landscape. Phase 1 (top): the boulders were still part of the Warton Sandstone lower cliff-line. Phase 2 (middle): large blocks separated and slowly slid down the slope. Phase 3 (bottom): Borologa 1 and 2 separated (see text for further details of each phase).

The presence down-slope of large blocks displaced from quartzite escarpments is often associated with the catastrophic collapse of cliff-lines (e.g. Young et al., 2009). Research undertaken on painted sites elsewhere in the Kimberley indicates that such collapsed blocks can continue to fragment afterwards, including after the arrival of people in the landscape by at least c. 50,000 years ago (e.g., see Delannoy et al., 2017). Our study on the Borologa sites signals a different cause for the translocation of boulders in this region. Here, the position and orientation of the blocks indicate their slow movement down the slope, rather than catastrophic falls down the hill. We found that blocks could be digitally refitted progressively down the slope, with both conjoining surfaces and stratigraphic matches clearly evident. The blocks retained their original orientations, and they did not roll, suggesting slow, reptational descents. Such movements are normally associated with loose and/or soft formations rather than rigid, hard rocks like quartzite. It is important here to consider the long timescales – many tens of thousands of years – in which these events took place, and the weathering processes that affected the less compact sandstone bedrock underfoot. The softening of quartzite surfaces through weathering ("ghost rock" formations) has been documented from many regions both in Australia and across the world (e.g., Armstrong et al., 2013; Delannoy et al., 2017; Martini & Grimes, 2012; Wray & Sauro, 2017). At Borologa, such weathering has mainly affected the exposed surfaces of bedrock pavements U–X (Fig. 7). Arenized (i.e., turned to sand) by weathering, the pavement surfaces acted like ball-bearings, allowing the

slow reptation from the lower cliff-line (E3) of large, detached blocks up to tens of metres long along the quartzitic slopes.

The only chronological data available for escarpment breakdown and boulder detachment relate to those from cliff-lines E1 and E2 shown in Figure 3. Cosmogenic ^{10}Be exposure dating places two such events within the range of a minimum c. 100,000–150,000 years ago, and up to a maximum age of as much as 500,000 years ago. Given that these cosmogenic nuclide ages pertain to the down-slope movement of the detached boulders from the upper quartzite cliff-faces, it may provide an upper limit to the emplacement of boulders at lower elevations to be less than 100,000–150,000 years ago. Hence the landing of Borologa 1–2 and Borologa 3–BR2 near the bottom of the slope is likely to have taken place at least many tens of thousands of years ago. These geomorphological observations and deductions indicate that the configuration of the present-day slope was probably similar to when ancestral populations first came to Borologa.

Three main phases of landscape evolution have thus been identified from the 3D retro-modelling (Fig. 15):

Phase 1: The boulders were not yet separated from the Warton Sandstone lower cliff-line, forming a large, continuous flat surface perched above the Drysdale River valley.

Phase 2: As the Drysdale River continued to incise the valley, the slopes slowly retreated, destabilising the Warton Sandstone cliff-face (E3). In doing so, retreat of the cliff-lines accelerated. Large blocks separated and slid down, coming to rest on an exposed quartzite pavement at the base of the slope.

Phase 3: Borologa 1 and 2 separated after they had reached their current location while still attached, with the smaller block (Borologa 2) tilting westward.

The 3D retrofitting and limited cosmogenic nuclide ages suggest that, at a landscape-scale, the Borologa hill-slope topography remained largely unchanged for many tens of thousands of

years. The large boulders we now see strewn across the slope have been in position for tens of thousands of years, and probably since before the first arrival of people in the Kimberley region. It is in this relatively stable topographic setting that the first settlers came to occupy the rock shelters and the overall landscape (e.g., David et al., 2019), flaked rock walls as stone quarries (e.g., Moore et al. 2020), actively hollowed out alcoves and overhangs (e.g., Delannoy et al., 2020a), and painted on and marked their rock surfaces (e.g., Finch et al. 2020; Gunn et al., 2019).

Acknowledgements

This research was supported by the "Kimberley Visions: Rock Art Style Provinces of North Australia" project (Australian Research Council LP150100490) administered by the University of Western Australia, in partnership with the Balanggarra Aboriginal Corporation, the Monash Indigenous Studies Centre at Monash University, the University of Melbourne and the Université Savoie Mont Blanc. Thank you to the Kimberley Foundation Australia and Dunkeld Pastoral for financial and logistic support. Individually, we thank: Maria and Cecilia Myers, Susan Bradley, Robin Maher and staff at Theda and Doongan Stations for logistical support and hospitality. The Western Australian Department of Biodiversity, Conservation and Attractions and the Department of Planning, Lands and Heritage are thanked for non-Aboriginal permits and permissions. K.G. was supported by a PhD scholarship from the Université Savoie Mont Blanc. We thank the Borologa excavation and rock art recording teams: Isaac Barney, Frank Boulden, Leigh Douglas, Adrian French, Paul Hartley, Brigid Hill, Lucas Karadada, Madeleine Kelly, Lorraine Lee, Robin Maher, William Maraltidj, Michael Morlumbin, Ken Mulvaney, Nick Sundblom, Patrick Tataya, Gareth Unghango, Jeremy Unghango, Scott Unghango, Ian Waina, Rowan Waina and Uriah Waina.

Data Sharing: Data sharing not applicable – no new data generated.

References

Armstrong, R., Osborne, L., Weliange, W. S., Jayasingha, P., Dandeniya, A. S., Algiriya, A. K. P. P., & Pogson, R. E. (2013). Caves and karst-like features in Proterozoic gneiss and Cambrian granite, southern and central Sri Lanka: An introduction. *Acta Carsologica*, 42(1), 25–48.

Bachmann, D., Bouissou, S., & Chemenda, A. (2009). Analysis of massif fracturing during deep-seated gravitational slope deformation by physical and numerical modeling. *Geomorphology*, 103, 130–135.

Ballesteros, D., Malard, A., Jeannin, P.-Y., Jiménez-Sánchez, M., García-Sansegundo, J., Meléndez-Asensio, M., & Sendra, G. (2015). KARSYS hydrogeological 3D modeling of alpine karst aquifers developed in geologically complex areas: Picos de Europa National Park (Spain). *Environmental Earth Sciences*, 74, 7699–7714. https://doi.org/10.1007/s12665-015-4712-0

Besl, P. J., & McKay, N. D. (1992). A method for registration of 3-D shapes. *IEEE Transactions on Pattern Analysis and Machine Intelligence*, 14, 239–256. https://doi.org/10.1109/34.121791

Braun, J. (2018). A review of numerical modeling studies of passive margin escarpments leading to a new analytical expression for the rate of escarpment migration velocity. *Gondwana Research*, 53, 209–224. https://doi.org/10.1016/j.gr.2017.04.012

Bronk Ramsey, C. (1995). Radiocarbon calibration and analysis of stratigraphy: The OxCal program. *Radiocarbon*, 37, 425–430.

Brunsden, D. (1999). Some geomorphological considerations for the future development of landslide models. *Geomorphology*, 30(1–2), 13–24. https://doi.org/10.1016/S0169-555X(99)00041-0

Campaña, I., Pérez-González, A., Benito-Calvo, A., Rosell, J., Blasco, R., de Castro, J.M.B., Carbonell, E., & Arsuaga, J.L. (2016). New interpretation of the Gran Dolina-TD6 bearing *Homo antecessor* deposits through sedimentological analysis. *Scientific Reports*, 6, 34799. https://doi.org/10.1038/srep34799

Carraro, F., Monego, M., Callegaro, C., Mazzariol, A., Perticarini, M., Menin, A., Achilli, V., Bonetto, J., & Giordano, A. (2019). The 3D survey of the roman bridge of San Lorenzo in Padova (Italy): A comparison between SFM and TLS methodologies applied to the arch structure. *International Archives of the Photogrammetry, Remote Sensing and Spatial Information Sciences*, XLII-2/W15, 255–262. https://doi.org/10.5194/isprs-archives-XLII-2-W15-255-2019

Cazes, G., Fink, D., Codilean, A. T., & Fülöp, R.-H. (2016). Spatial pattern of denudation in a lithologically controlled sub-tropical flat landscape: Insights from the Kimberley region, NW Australia. *Geophysical Research Abstracts*, 18. https://doi.org/10.13140/rg.2.1.2911.7043

Cazes, G., Fink, D., Codilean, A. T., Fülöp, R.-H., Fujioka, T., & Wilcken, K. M. (2020). $^{26}Al/^{10}Be$ ratios reveal the source of river sediments in the Kimberley, NW Australia. *Earth Surface Processes and Landforms*, 45, 424–439. https://doi.org/10.1002/esp.4744

Clarkson, C., Marwick, B., Fullagar, R., Wallis, L., Smith, M., Roberts, R. G., Hayes, E., Lowe, K., Carah, X., Florin, S. A., McNeil, J., Cox, D., Arnold, L. J., Hua, Q., Huntley, J., Brand, H. E. A., Manne, T., Fairbairn, A., Shulmeister, J., Lyle, L., Salinas, M., Page, M., Connell, K., Park, G., Norman, K., Murphy, T., & Pardoe, C.

(2017). Human occupation of northern Australia by 65,000 years ago. *Nature*, 547, 306–310.

Crozier, M. J. (2010). Landslide geomorphology: An argument for recognition, with examples from New Zealand. *Geomorphology*, 120 (1–2), 3–15. https://doi.org/10.1016/j.geomorph.2009.09.010

Danielson, J. J., & Gesch, D. B. (2011). *Global multi-resolution terrain elevation data 2010 (GMTED2010)*. Sioux Falls: US Geological Survey.

David, B., Delannoy, J.-J., Petchey, F., Gunn, R., Huntley, J., Veth, P., Genuite, K., Skelly, R. J., Mialanes, J., Harper, S., Ouzman, S., Balanggarra Aboriginal Corporation, Heaney, P., & Wong, V. (2019). Dating painting events through by-products of ochre processing: Borologa 1 Rockshelter, Kimberley, Australia. *Australian Archaeology*, 85, 57–94.

David, B., Hogan, P., Walt, H., Wilson, M., McNiven, I. J., & Lawson, E. (2005). Rio de las Vacas Shelter and the distribution of Sudden and San Rafael Side-notched points: High country cultural links during the late Archaic in the American Southwest. *The Artefact*, 27, 113–122.

David, B., & Lourandos, H. (1997). 37,000 years and more in tropical Australia: investigating long-term archaeological trends in Cape York Peninsula. *Proceedings of the Prehistoric Society*, 63, 1–23.

Delannoy, J.-J., David, B., Geneste, J.-M., Katherine, M., Barker, B., Whear, R. L., & Gunn, R. G. (2013). The social construction of caves and rockshelters: Chauvet Cave (France) and Nawarla Gabarnmang (Australia). *Antiquity*, 87, 12–29. https://doi.org/10.1017/S0003598X00048596

Delannoy, J.-J., David, B., Geneste, J.-M., Katherine, M., Sadier, B., & Gunn, R. (2017). Engineers of the Arnhem Land plateau: Evidence for the origins and transformation of

sheltered spaces at Nawarla Gabarnmang. In B. David, J.-J. Delannoy, J.-M. Geneste & P. Taçon (Eds), *The Archaeology of rock art in western Arnhem land, Australia* (pp. 197–243). Terra Australis 47. Canberra: ANU Press.

Delannoy, J.-J., David, B., Fresløv, J., Mullett, R., GunaiKurnai Land and Waters Aboriginal Corporation, Green, H., Berthet, J., Petchey, F., Arnold, L.J., Wood, R., McDowell, M., Crouch, J., Mialanes, J., Ash, J., & Wong, V.N.L. (2020b). Geomorphological context and formation history of Cloggs Cave: What was the cave like when people inhabited it? *Journal of Archaeological Science: Reports*, 33, 102461. https://doi.org/10.1016/j.jasrep.2020.102461

Delannoy, J.-J., David, B., Genuite, K., Gunn, R., Finch, D., Ouzman, S., Green, H., Veth, P., Harper, S., Balanggarra Aboriginal Corporation, & Skelly, R. (2020a). Investigating the construction of rock art sites through archaeomorphology: The case of Borologa, Kimberley, Australia. *Journal of Archaeological Method and Theory*, 27, 631–669. https://doi.org/10.1007/s10816-020-09477-4

Delannoy, J.-J., Deline, P., & Lhénaff, R. (2016). *Géographie Physique: Aspects et Dynamique du Géosystème Terrestre*. Paris: Vuibert Editions.

Delaunay, B. (1934). Sur la sphère vide: A la mémoire de Georges Voronoi. *Bulletin de l'Académie des Sciences de l'URSS*, 6, 793–800.

De Vita, P., Carratù, M. T., La Barbera, G., & Santoro, S. (2013). Kinematics and geological constraints of the slow-moving Pisciotta rock slide (southern Italy). *Geomorphology*, 201, 415–429.

Doneus, M., Briese, C., Fera, M., & Janner, M. (2008). Archaeological prospection of forested areas using full-waveform airborne laser scanning. *Journal of Archaeological Science*, 35, 882–893. https://doi.org/10.1016/j.jas.2007.06.013

Doring, J. (Ed.) (2000). *Gwion gwion: the secret and sacred pathways of the Ngarinyin Aboriginal people of Australia*. Köln: Konemann Verlagsgesellschaft

Douillard, B., Underwood, J., Kuntz, N., Vlaskine, V., Quadros, A., Morton, P., & Frenkel, A. (2011). On the segmentation of 3D LIDAR point clouds. In *2011 IEEE International Conference on Robotics and Automation*, pp. 2798–2805. https://doi.org/10.1109/ICRA.2011.5979818

Duvillard, P.-A., Ravanel, L., Deline, P., & Dubois, L. (2018). Paraglacial rock slope adjustment beneath a high mountain infrastructure — The Pilatte Hut case study (Écrins mountain range, France). *Frontiers in Earth Science*, 6. https://doi.org/10.3389/feart.2018.00094

Finch, D., Gleadow, A., Hergt, J., Levchenko, V. A., Heaney, P., Veth, P., Harper, S., Ouzman, S., Myers, C., & Green, H. (2020). 12,000-year-old Aboriginal rock art from the Kimberley region, Western Australia. *Science Advances*, 6(6): eaay3922. https://doi.org/10.1126/sciadv.aay3922

Gamble, C. (1994). *Timewalkers: the prehistory of global colonization*. Cambridge: Harvard University Press.

Girardeau, D. (2018). *CloudCompare: 3D point cloud and mesh processing software, Open Source Project*. https://www.danielgm.net/cc/

Godard, V., Dosseto, A., Fleury, J., Bellier, O., & Siame, L. (2019). Transient landscape dynamics across the Southeastern Australian Escarpment. *Earth and Planetary Science Letters*, 506, 397–406. https://doi.org/10.1016/j.epsl.2018.11.017

Gomes, A., Voiculescu, I., Jorge, J., Wyvill, B., & Galbraith, C. (2009). *Implicit curves and surfaces: mathematics, data structures and algorithms*. London: Springer-Verlag.

Gunn, R., David, B., Douglas, L., Delannoy, J.-J., Harper, S., Heaney, P. Ouzman, S., & Veth, P. (2019). 'Kimberley Stout figures': a new rock art style for Kimberley rock art, north-western Australia. *Australian Archaeology*, 85, 151–169.

Harper, S., Veth, P., & Ouzman, S. (2020). Kimberley rock art. In C. Smith (Ed.), *Encyclopedia of Global Archaeology*. Cham: Springer. https://doi.org/10.1007/978-3-319-51726-1_3449-1

Ilic, S. (2005). Implicit meshes unifying implicit and explicit surface representations for 3D reconstruction and tracking. *Infoscience*. https://doi.org/10.5075/epfl-thesis-3243

Jaillet, S., Delannoy, J.-J., Monney, J., & Sadier, B. (2017). 3-D modelling in rock art research: terrestrial laser scanning, photogrammetry and the time factor. In B. David and I. J. McNiven (Eds), *The Oxford handbook of the archaeology and anthropology of rock art*. https://www.oxfordhandbooks.com/view/10.1093/oxfordhb/9780190607357.001.0001/oxfordhb-9780190607357-e-45

James, M.R., Robson, S., & Smith, M.W. (2017). 3-D uncertainty-based topographic change detection with structure-from-motion photogrammetry: Precision maps for ground control and directly georeferenced surveys. *Earth Surface Processes and Landforms*, 42, 1769–1788. https://doi.org/10.1002/esp.4125

Jaubert J., Verheyden, S., Genty, D., Soulier, M., Cheng, H., Blamart, D., Burlet, C., Camus, H., Delaby, S., Deldicque, D., Edwards, R. L., Ferrier, C., Lacrampe-Cuyaubère, F., Lévêque, F., Maksud, F., Mora, P., Muth, X., Régnier, E., Rouzaud, J.-N., & Santos, F. (2016). Early Neanderthal constructions deep in Bruniquel Cave in southwestern France. *Nature*, 534, 111–114. https://www.nature.com/articles/nature18291

Kolbe, T. H., König, G., & Nagel, C. (2011). *Advances in 3D geo-information sciences*. London: Springer-Verlag.

Lin, X., & Zhang, J. (2014). Segmentation-based filtering of airborne LiDAR point clouds by progressive densification of terrain segments. *Remote Sensing*, 6, 1294–1326. https://doi.org/10.3390/rs6021294

Lourandos, H. (1983). Intensification: a late Pleistocene–Holocene archaeological sequence from south-western Victoria. *Archaeology in Oceania*, 18, 81–94.

Martini J. E. J., & Grimes, K. G. (2012). Epikarst maze cave development: Bullita Cave system, Judbarra/Gregory karst, tropical Australia. *Helictite*, 41, 37–66.

Maur, P. (2002). *Delaunay triangulation in 3D*. https://www.kiv.zcu.cz/site/documents/verejne/vyzkum/publikace/technicke-zpravy/2002/tr-2002-02.pdf

Mitášová, H., & Hofierka, J. (1993). Interpolation by regularized spline with tension: II. Application to terrain modeling and surface geometry analysis. *Mathematical Geology*, 25, 657–669. https://doi.org/10.1007/BF00893172

Moore, M. W., Westaway, K., Ross, J., Newman, K., Perston, Y., Huntley, J., Keats, S., Kandiwal Aboriginal Corporation, Morwood, M. J. (2020). Archaeology and art in context: Excavations at the Gunu Site Complex, northwest Kimberley, Western Australia. *PlosOne*, 15(2), e0226628. https://doi.org/10.1371/journal.pone.0226628

Nott, J., Young, R., & McDougall, I. (1996). Wearing down, wearing back, and gorge extension in the long-term denudation of a highland mass: quantitative evidence from the Shoalhaven Catchment, southeast Australia. *The Journal of Geology*, 104, 224–232. https://doi.org/10.1086/629816

Opitz, R., & Nuninger, L. (2013). Point cloud metrics for separating standing archaeological remains and low vegetation in ALS data. *International Archives of the Photogrammetry, Remote Sensing and Spatial Information Sciences*, XL-5/W2.

https://www.int-arch-photogramm-remote-sens-spatial-inf-sci.net/XL-5-W2/459/2013/isprsarchives-XL-5-W2-459-2013.pdf

Reimer, P. J., Bard, E., Bayliss, A., Beck, J. W., Blackwell, P. G., Bronk Ramsey, C., Buck, C. E., Cheng, H., Edwards, R. L., Friedrich, M., Grootes, P. M., Guilderson, T. P., Hajdas, I., Hatté, C., Heaton, T. J., Hoffman, D., Hogg, A. G., Hughen, K. A., Kaiser, K. F., Kromer, B., Manning, S. W., Niu, M., Reimer, R. W., Richards, D. A., Scott, E. M., Southon, J. R., Staff, R. A., Turney, C. S. A., & van der Plicht, J. (2013). IntCal13 and marine13 radiocarbon age calibration curves, 0–50,000 years cal BP. *Radiocarbon*, 55(4), 1869–1887.

Remondino, F. (2003). From point cloud to surface: the modeling and visualization problem. International Archives of the Photogrammetry, Remote Sensing and Spatial Information Sciences, XXXIV-5/W10. https://www.isprs.org/proceedings/xxxiv/5-W10/papers/remondin.pdf

Remondino, F., & Campana, S. (Eds) (2014). *3D recording and modelling in archaeology and cultural heritage: theory and best practices*. Oxford: British Archaeological Reports. https://doi.org/10.30861/9781407312309

Sadier, B., Delannoy, J.-J., Benedetti, L., Bourles, D.L., Jaillet, S., Geneste, J.-M., Lebatard, A.-E., & Arnold, M. (2012). Further constraints on the Chauvet cave artwork elaboration. *Proceedings of the National Academy of Sciences of the United States of America*, 109, 8002–8006. https://doi.org/10.1073/pnas.1118593109

Sharp, G. C., Lee, S. W., & Wehe, D. K. (2002). ICP registration using invariant features. *IEEE Transactions on Pattern Analysis and Machine Intelligence*, 24, 90–102. https://doi.org/10.1109/34.982886

Shi, Q., Xi, N., Chen, Y., & Sheng, W. (2006). Registration of point clouds for 3D shape inspection. *2006 IEEE/RSJ International Conference on Intelligent Robots and Systems*, pp. 235–240. https://doi.org/10.1109/IROS.2006.281677

Sithole, G., & Vosselman, G. (2005). Filtering of airborne laser scanner data based on segmented point clouds. http://citeseerx.ist.psu.edu/viewdoc/download?doi=10.1.1.222.1923&rep=rep1&type=pdf

Verhoeven, G. J. (2017). Mesh is more—using all geometric dimensions for the archaeological analysis and interpretative mapping of 3D surfaces. *Journal of Archaeological Method and Theory*, 24, 999–1033. https://doi.org/10.1007/s10816-016-9305-z

Veth, P., Ditchfield, K., Bateman, M., Ouzman, S., Benoit, M., Motta, A. P., Darrel, L., Harper, S., & Balanggarra Aboriginal Corporation (2019). Minjiwarra: archaeological evidence of human occupation of Australia's northern Kimberley by 50,000 BP: *Australian Archaeology*, 85, 115–125. https://doi.org/10.1080/03122417.2019.1650479

Wray, R. A. L. (1997). Quartzite dissolution: karst or pseudokarst? *Cave and Karst Science*, 24, 81–86.

Wray, R. A. L., & Sauro, F. (2017). An updated global review of solutional weathering processes and forms in quartz sandstones and quartzites. *Earth Sciences Reviews*, 171, 520–557. http://dx.doi.org/10.1016/j.earscirev.2017.06.008

Young, R. W. (1987). Sandstone landforms of the tropical East Kimberley region, northwestern Australia. *The Journal of Geology*, 95, 205–218. https://doi.org/10.1086/629120

Young, R. W., Wray, R. A. L., & Young, A. R. M. (2009). *Sandstone Landforms*. New York: Cambridge University Press.

Appendix A. Correlation values for the 3D conjoined blocks. The RMSE values represent the ICP best-fit results computed from the paired point clouds. When RMSE correlations could not be obtained, e.g. because of insufficient data or excessive surface weathering, correlations were visually assessed through direct inspection and stratigraphic matches on the 3D model.

Conjoins (blocks)	Strata correlate	Surface morphologies correlate	Computed points	RMSE (m)	Block clusters	Quality assessment
B1–B2	yes	yes	49,999	0.024	Borologa 1–2	High
A1–A2	yes	yes	2290	0.021	B	High
J–K	yes	yes	1904	0.007	G	High
I–(J–K)	yes	yes	5545	0.022	G	High
G–H	yes	yes	2918	0.007	C	High
(A1–2)–B1	yes	yes	_	visual	B	Medium
B–B1	yes	yes	9661	0.046	B	High
A1–E	yes	yes	3918	0.042	B	High
B–C	yes	yes	_	visual	B	Medium
C–D	yes	yes	_	visual	B	Medium

N–O	no	yes	_	visual	F	Low
O–P	no	yes	_	visual	F	Low
P–Q	no	no	_	visual	H	Very Low
Q–R	no	no	_	visual	H	Very Low
S–T	yes	yes	_	visual	H	Medium
S–U	yes	yes	_	visual	H	Medium
V–W	yes	yes	1255	0.029	D	High
V–X	yes	yes	_	visual	D	Medium
Z–Ax	yes	yes	_	visual	F	Medium
BR1–BR2	yes	no	_	_	Borologa 3	Low
Cx–Dx	yes	yes	_	visual	E	Medium
Dx–Ex	yes	yes	9722	0.008	E	High
Cx–Ex	yes	yes	_	visual	E	Medium
Ex–Fx	yes	yes	20,615	0.02	E	High